4.1. Best standard parameters for the preparation of chitosan nanoparticles

4.1.1. Formulation variables

4.1.1.1. Effect of polymer concentration on particle size and drug entrapment efficiency of nanoparticle.

The various parameters that were optimized for obtaining maximum encapsulation efficiency along with smaller size of the nanoparticles, included, chitosan concentration, TPP concentration, stirring speed and stirring time. In chitosan concentration optimization (Table.11), four different concentrations of chitosan were studied for synthesis of nanoparticles i.e. 1, 2, 3 and 4 mg/ml, while other factors such as cross linker concentration and stirring time were kept constant. Effect of polymer concentration was observed with the results that the average particle size and encapsulation efficiency varied from 104-725nm and 40-75%, respectively (Table 11). Similar particle size range with insulin loaded chitosan nanoparticles were obtained by Avadi et al., 2010. The best particle size along with maximum encapsulation efficiency was found at 1mg/ml. Impact of different concentrations of cross linker was further studied at this optimized chitosan concentration. It was inferred that with increase in chitosan concentration viscosity of the solution increases, which in turn results in bigger size nanoparticles (Thiaune et al., 1997).

Serial No.	Cross-linking agent concentration (%)	Polymer concentration mg/ml	Average particle size (nm)	Drug entrapment efficiency (%)
1.	0.85	1	104±57.27	75.2±6.2
2.	0.85	2	333±68.01	64.5±5.4
3.	0.85	3	496±55.0	52.4±7.6
4.	0.85	4	725±61.8	40±8.33

Table.11: Effect of polymer concentration on particle size and drug entrapment efficiency of nanoparticle. The results were expressed as mean ±standard deviation (SD, n = 3).

4.1.1.2. Effect of cross-linking agent concentration on particle size and drug entrapment efficiency of nanoparticle.

Tripolyphosphhate (cross-linker) concentration optimization - At the best chitosan concentration, three different concentrations of TPP (0.25%, 0.5%, 0.75%, and 1%) were tested (Table.12), while keeping stirring rate and stirring time constant. Cross linker with concentration of 0.75%, maximized the encapsulation giving a maximum encapsulation efficiency of 77±8.2% and particle size of 130±45.7nm. Impact of different stirring durations was studied at these polymer and cross-linker concentrations. If the concentration of polyanion decreases or increases from 0.75% the gradual increase in particle size was observed which could be due to formation of micellar structure of chitosan with decrease in surface tension and development of charge over the particle due to presence of TPP (Ahlin et al., 2002). Similar particle size range with insulin loaded chitosan nanoparticles were obtained by Avadi et al., 2010.

Serial No.	Cross-linking agent concentration (%)	Polymer concentration (mg/ml)	Average particle size (nm)	Drug entrapment (%)
1.	0.25	1	469±54.0	41±9.8
2.	0.50	1	320±57.0	63±6.6
3.	0.75	1	130±45.7	77±8.2
4.	1.00	1	143±63.05	72.5±6.6

Table.12: Effect of cross-linking agent concentration on the particle size and drug entrapment efficiency of nanoparticle. The results were expressed as mean ±standard deviation (SD, n = 3).

4.1.2. Process variables

4.1.2.1. Effect of stirring speed on particle size and drug entrapment efficiency of nanoparticle.

All the samples were studied in triplicate and results were expressed as standard deviation, mean. Effect of stirring speed on particle size was also observed for four different rates i.e. 250, 500, 750 and 1000 rpm at best polymer (chitosan) and cross linker (TPP) concentration. Stirring speed of 500 rpm was observed to be most suitable with highest entrapment efficiency i.e. 77±7.5% and minimum particle size of 137±52nm (Table.13). At the optimum stirring speed of 500 rpm the particle size was decreased, but before and after this value the particle size increased and drug entrapment efficiency decreased due to development of charge over nanoparticles and aggregation of particles. Similar particle size range but different entrapment efficiency at 500 rpm was observed by Ahlin et al., 2002 & Hussain et al., 2016.

Serial No.	Stirring speed (rpm)	Average particle size(nm)	Drug entrapment efficiency (%)
1.	250	232±54.8	64±10.4
2.	500	137±52.0	77±7.5
3.	750	245±65	63±8.4
4.	1000	339±60	42±10.3

Table.13: Effect of stirring speed on particle size and drug entrapment efficiency of nanoparticle. The results were expressed as mean ±standard deviation (SD, n = 3).

4.1.2.2. Effect of stirring time on particle size and drug entrapment efficiency of nanoparticle.

Effect of stirring time on particle size was also observed for four different durations i.e. 30, 60, 90 and 120 mins at best polymer (chitosan) and cross linker (TPP) concentration. Stirring time of 60 mins was observed to be most suitable with highest entrapment efficiency i.e. 75.2±6.2% and minimum particle size of 132±51.4nm (Table.14). At optimum stirring time of 60 mins the particle size decreased, but increased at lower and higher values due to aggregation of particles and development of charge over the nanoparticles. Hussain et al., 2016 observed highest particle size with higher entrapment efficiency at 30 mins.

Serial no.	Stirring speed(mins)	Average particle size(nm)	Drug entrapement(%)
1.	30	437±62.01nm	53.7±7.3
2.	60	132±51.4nm	75.2±6.2
3.	90	230±37.8nm	67±8.8
4.	120	254±20.5nm	62±7.05

Table.14: Effect of stirring time on particle size and drug entrapment efficiency of nanoparticle. The results were expressed as mean ±standard deviation (SD, n = 3).

4.2. Characterization of Amphotericin B loaded Chitosan nanoparticles

4.2.1. Measurement of Particle size & Morphology Study

It was evident from the SEM study of nanoparticles that the size ranges 40-70 nm for the CS1 formulation and with the increase in chitosan concentration size of nanoparticles also increased. The most satisfactory nanoparticles of chitosan were obtained at a chitosan concentration of 1mg/ml in 1% acetic acid and TPP of 0.85% (w/v) in D/W. Nanoparticles with uniform and spherical morphology with clear surface were observed (Figure 15). SEM images also revealed that the nanoparticles were not aggregated and the size was found to be optimum for the oral delivery of Amphotericin B. Nanoparticles size range above 400nm for the same drug loaded with chitosan nanoparticles were obtained by Chauhan et al., 2016.

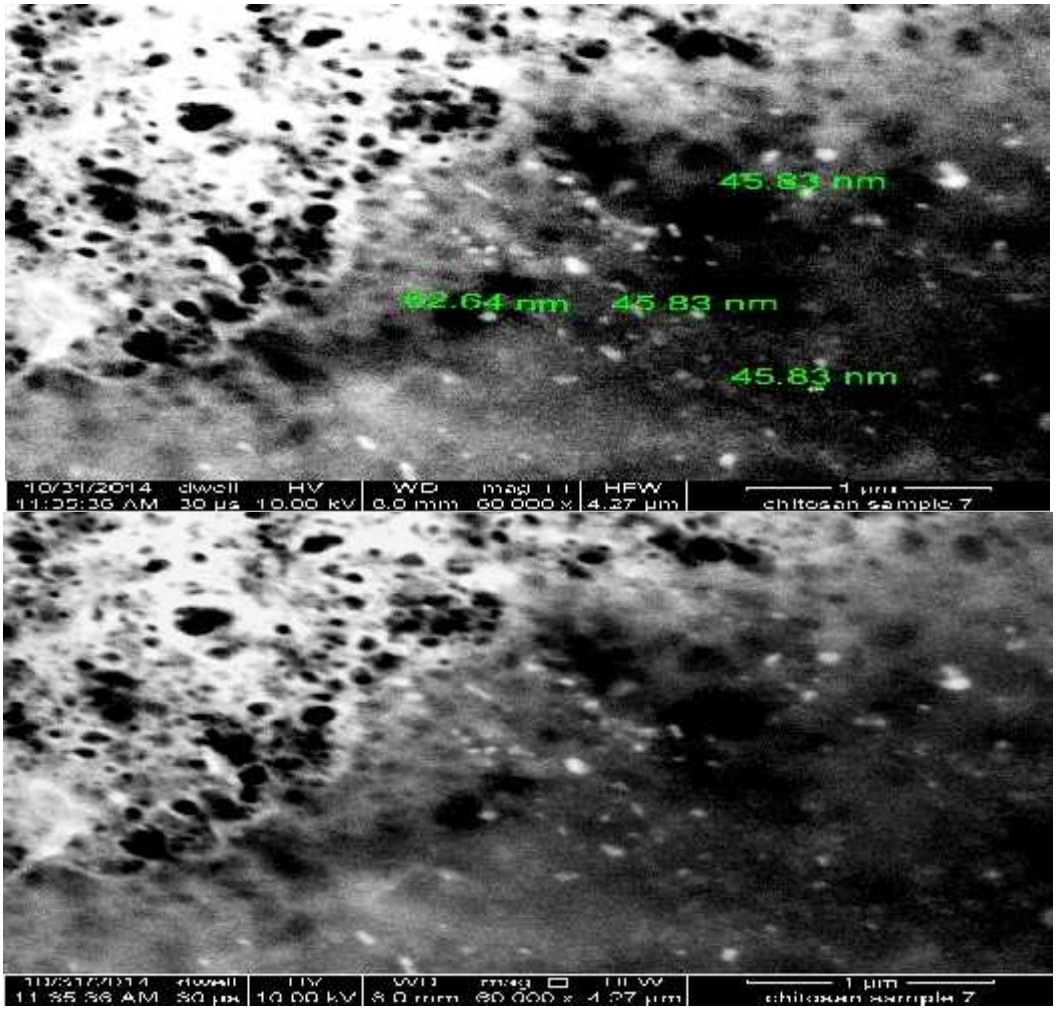

Figure.15: SEM images of chitosan nanoparticles (CS1) loaded with Amphotericin B, a poorly soluble drug.

4.2.2. Entrapment Efficiency and Percentage Yield of Amphotericin B loaded chitosan nanoparticles formulations

With the increasing concentration of chitosan the Amphotericin B entrapment efficiency decreased due to increase in viscosity of solution that leads to hindrance in particle movement and thus decreases in particle size. The results of entrapment efficiency revealed that drug entrapment efficiency (%EE) was dependent on the polymer concentration (Fig 16). The entrapment efficiency was found to be maximum for the CS1 formulation where chitosan concentration was kept minimum i.e. 1 mg/ml. Due to decrease in particle size the surface area of chitosan nanoparticles was increased which in turn results in higher drug entrapment efficiency. Percentage yield of 39.04 % was obtained for CS1 formulation of Amphotericin B.

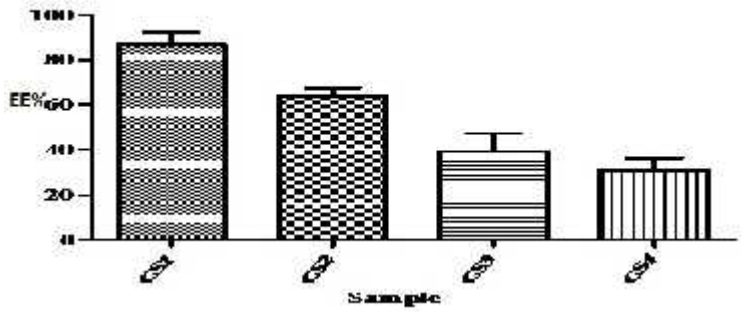

Figure.16: Bar diagram showing effect of chitosan concentration on Amphotericin B entrapment efficiency (%EE) of nano-formulations (CS1, CS2, CS3 & CS4) at physiological pH and temperature. The error bar indicates the standard deviation averaged from three measurements.

4.2.3. Comparative study of cumulative *in-vitro* drug release profile of Amphotericin B

The % cumulative release of free drug was showing a biphasic release pattern where around 60 % of free drug release in just 1h and remaining in around 9 h (Fig 17). The drug from CS1 formulation and thiolated chitosan formulation was showing a sustained release pattern for up to 9 h that is a continuous release of drug up to certain period of time i.e.10 h. Some other formulations of Amphotericin B like ambisome and fungisome available in market but they have the toxicity issues (Adler-Moore et al., 2016).

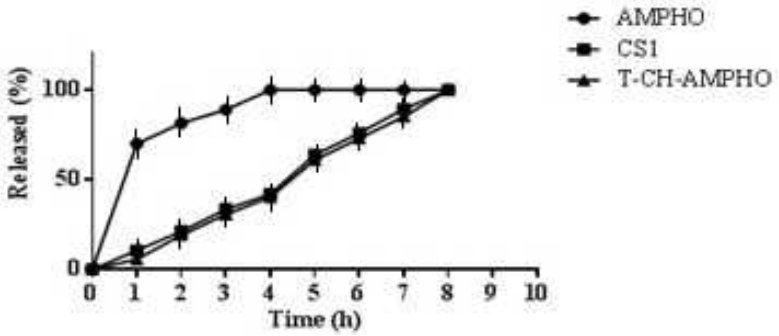

Figure.17: Cumulative drug release percentage profile of free Amphotericin B (AMPHO) & Amphotericin B from chitosan nanoparticle (CS1) & thiolated chitosan (T-CH-AMPHO) formulation up to 10 h at physiological pH and temperature.

4.2.4. Fourier-Transform Infra-Red Spectroscopy

The FTIR spectra of pure chitosan fig 18 (a), chitosan nanoparticles fig 18 (b) and Amphotericin B loaded chitosan nanoparticles (CS1) fig 18 (c) shown. In the chitosan spectra, the strong and wide peak in the 3500-3300 area was mainly because of the O-H bonding stretching vibration. The peaks of N-H stretching from primary amine as well as type II amide were overlapped in the same region. The asymmetric stretch peak of C-O-C was found around at 1150 cm^{-1} and the peak at 1317 cm^{-1} belongs to the type 1 amine C-N stretching vibration. In chitosan-TPP nanoparticles the tip of the peak of 3438 cm^{-1} had a shift to 3320 cm^{-1} and also becomes wider with increased relative intensity indicating increase in hydrogen bonding. In nanoparticles the peaks for N-H bending vibration of amine I at 1600 cm^{-1} and the amide II carbonyl stretch at 1650 cm^{-1} shifted to 1540 cm^{-1} and 1630 cm^{-1}, respectively. The cross-linked chitosan also showed a P=O peak at 1170 cm^{-1}. This result corresponds to the linkage of phosphoric group of TPP and ammonium ion of chitosan (Mohammadpour et al., 2012). In Amphotericin B loaded chitosan nanoparticle spectra, no changes in peaks observed that confirmed that the Amphotericin B was entrapped in the chitosan matrix without any chemical linkage (Mohammadpour et al., 2012).

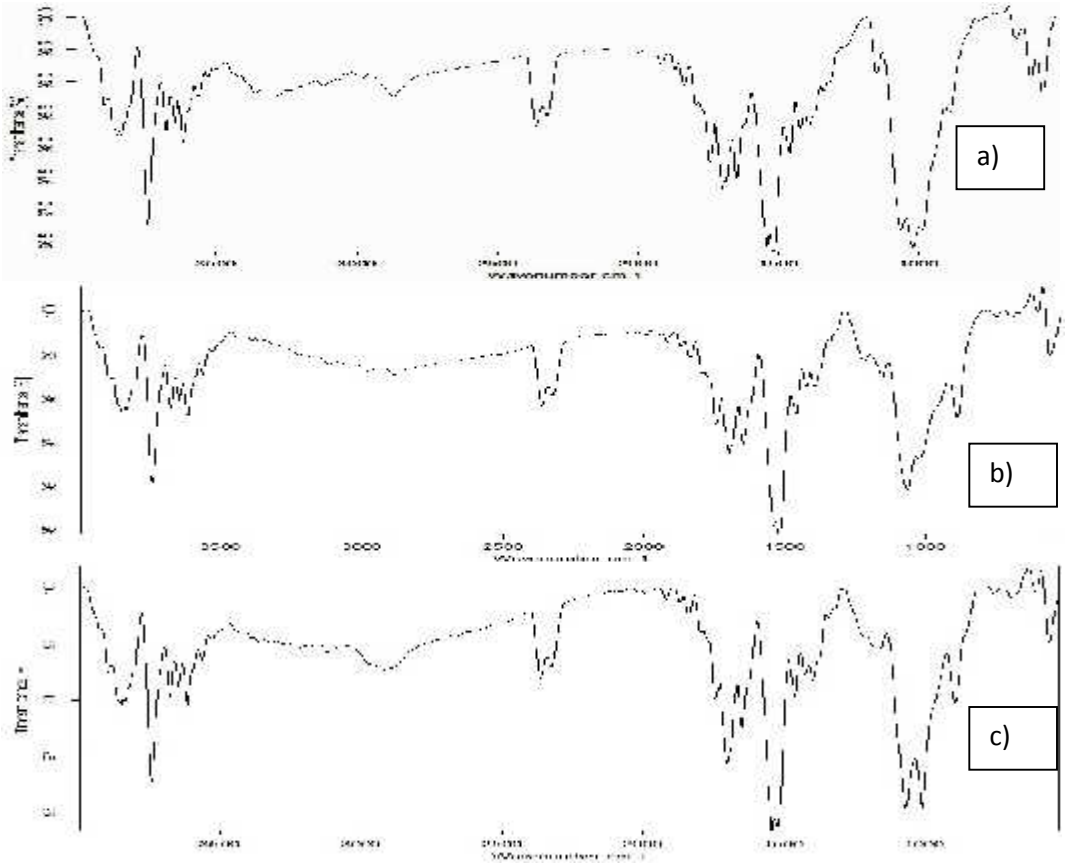

Figure.18 (a), (b), (c): FTIR analysis shows (a) chitosan and (b) chitosan-TPP nanoparticles and (c) chitosan nanoparticles loaded with Amphotericin B (CS1).

4.2.5. X-Ray Crystallography

The crystalline or amorphous phase identification of the studied sample (CS1) was carried out using X-ray diffraction (XRD). It is a non-destructive technique widely used for the characterization of crystalline/amorphous nature of the materials. The XRD spectra of the chitosan fig 19 (a), chitosan nanoparticles fig 19 (b), pure Amphotericin B fig 19 (c) and Amphotericin B containing chitosan nanoparticles fig 19 (d) were determined (Figure. 19). XRD patterns of chitosan, chitosan nanoparticles and pure Amphotericin B showed peaks at 2θ-scattered angles of 20 to 30; these peaks were indicating the semicrystalline nature of chitosan, chitosan nanoparticles and polycrystalline nature of pure Amphotericin B. Peaks of Amphotericin B disappeared in Amphotericin B loaded chitosan nanoparticles (CS1) (Wang et al., 2016). This confirmed that the Amphotericin B present in the core of chitosan nanoparticles in amorphous state that leads to increase in its solubility. This pattern of XRD was also investigated by other scientists with drug Niclosamide (Naqvi et al., 2017).

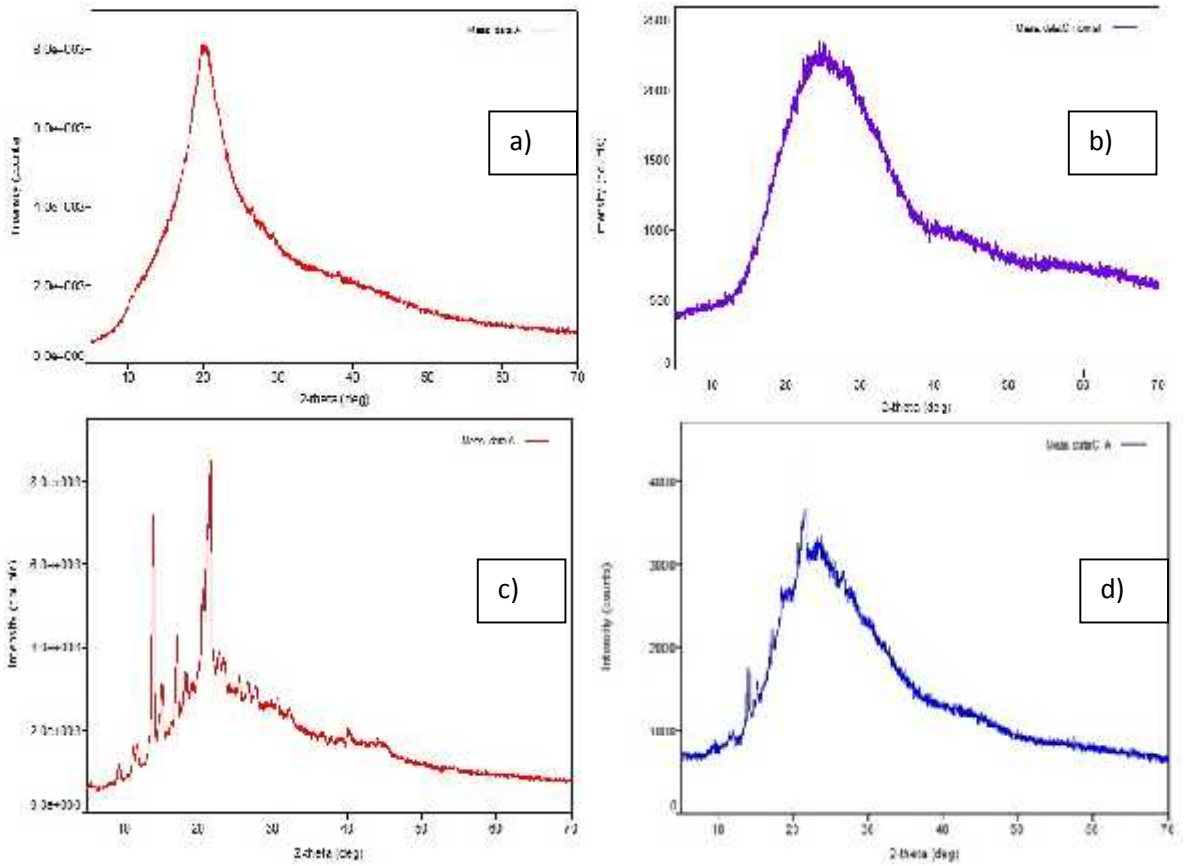

Figure.19: XRD spectra of a) pure chitosan, b) chitosan nanoparticles, c) pure Amphotericin B and d) Amphotericin B loaded chitosan nanoparticles (CS1).

4.2.6. Zeta-potential analysis of Amphotericin B loaded chitosan nanoparticles

Zeta potential value for the Amphotericin B loaded chitosan nanoparticle (CS1) was found to be +24.2 mV (Figure. 20). Zeta potential values provide an important criterion for the stability of colloidal system and the surface charge. The higher the particles are equally charged, the greater is the electrostatic repulsion between the particles and longer is the physical stability. This was the electric potential that exists at the shear plane of a particle, which was related to both the surface charge and local environment of the nanoparticle. The positive value of zeta potential indicated positive charge on the surface of Amphotericn B loaded chitosan nanoparticles which results in better cytotoxity and uptake of nanoparticles by negatively charged peptidoglycan cell membrane with greater stability (Fröhlich et al., 2012). This positive charge on the surface of Amphoterin B loaded chitosan nanoparticle formulation CS1 might be due to presence of unreacted NH_2 groups available on chitosan surface for attachment to other negatively charged molecule. Other scientists also obtained zeta potential ranging +22 to +55mV for stable chitosan nanoparticles (Yien et al., 2012).

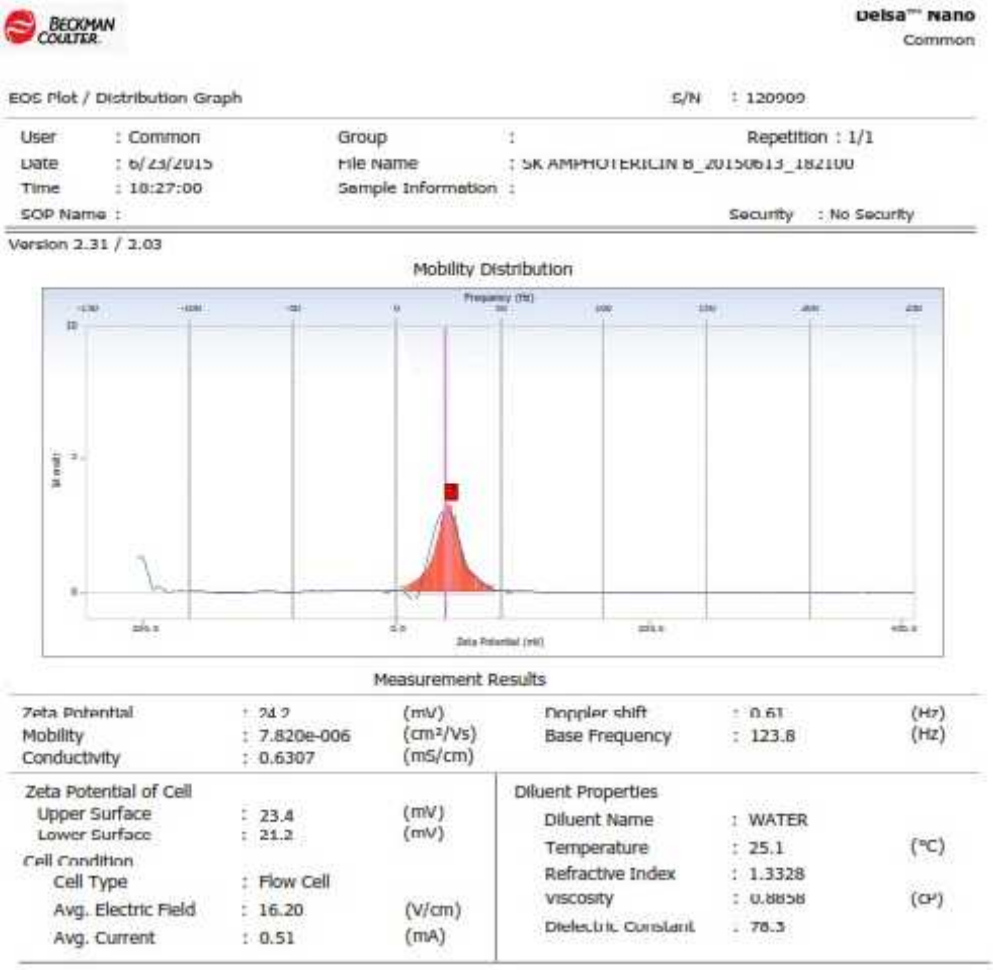

Figure.20: Zeta potential distribution plot for Amphotericin B loaded chitosan nanoparticles (CS1).

4.2.7. Antimicrobial study

The microbiological studies were carried out to ascertain the antifungal activity of the prepared formulation and compared with the free drug activity. Figure.21 indicated that test preparations containing the Amphotericin B loaded chitosan nanoparticles and free Amphotericin B demonstrated that zone of inhibition (12mm) was seen in both the cases for up to 48h of incubation against *A. fumigatus* (sensitive to Amphotericin B). The commercial preparations of Amphotericin B in comparison to the Amphotericin B loaded chitosan nanoparticles exhibited similar antimicrobial activity within 48h (Ibrahim et al., 2012). Therefore it could be said that the antifungal effect or activity of this drug was not at all affected after getting entrapped in the chitosan matrix.

Figure.21: Zone of Clearance in the lawn of *Aspergillus fumigatus* by a) free drug and b) drug loaded chitosan nanoparticle after 48h of Incubation.

4.3. Characterization of Ketoconazole loaded chitosan nanoparticles

4.3.1. Measurement of Particle size & Morphology Study

The most satisfactory nanoparticles of chitosan were obtained at a chitosan concentration of 1mg/ml in 1% acetic acid and TPP of 0.85% (w/v) in D/W. It was evident from the SEM study of nanoparticles that the size ranges from 50-80 nm for the CS1 formulation of Ketoconazole and with the increase in chitosan concentration size of nanoparticles also increased. Further, clear surface with uniform spherical morphology was observed (Figure. 22). SEM images also revealed that the chitosan nanoparticles were seen without aggregation and the size range obtained was found to be optimum for the oral delivery of Ketoconazole (Paralikar., 2015).

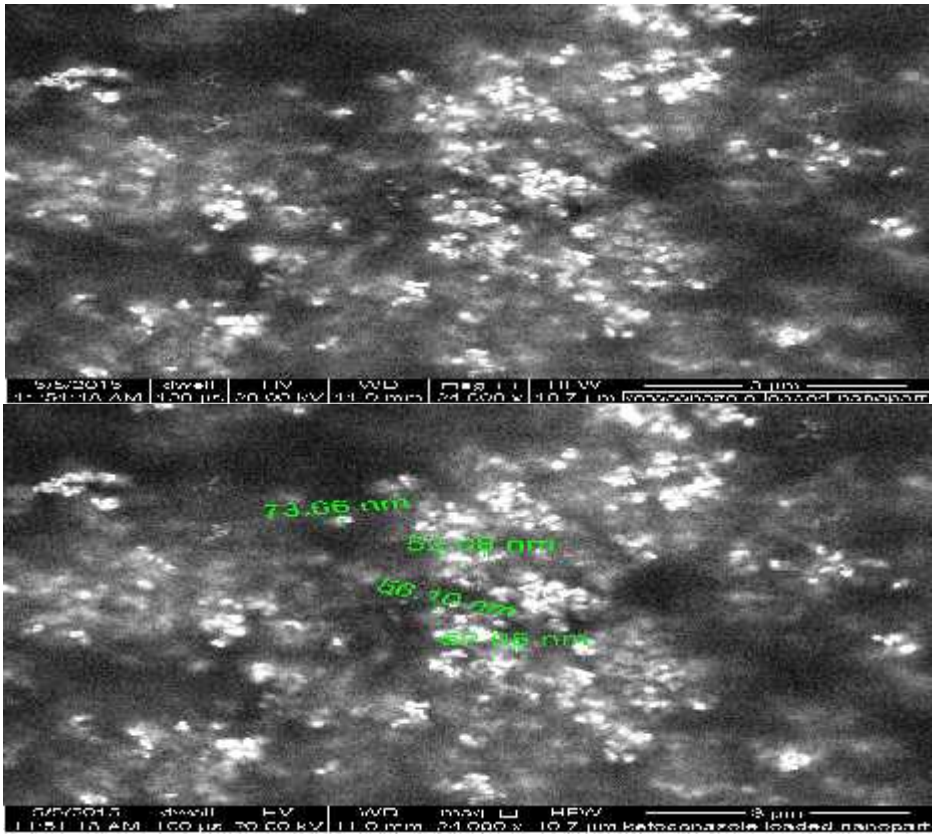

Figure.22: SEM images of chitosan nanoparticles loaded with Ketoconazole, a poorly soluble drug.

4.3.2. Entrapment efficiency and Percentage Yield of Ketoconazole loaded chitosan nanoparticle formulations

The results of entrapment efficiency revealed that Ketoconazole entrapment efficiency in chitosan nanoparticles was dependent on the polymer concentration. The entrapment efficiency was found to be maximum for the CS1 formulation of Ketoconazole where chitosan concentration was kept lowest i.e. 1 mg/ml (Fig 23). With the increasing concentration of chitosan the drug entrapment efficiency decreased due to increase in viscosity of solution that

leads to hindrance in particle movement and thus decreases in particle size. Due to decrease in particle size the surface area of chitosan nanoparticles was increased which in turn resulted in higher drug entrapment efficiency. Percentage yield of 39.04 % was obtained for CS1 formulation of Ketoconazole.

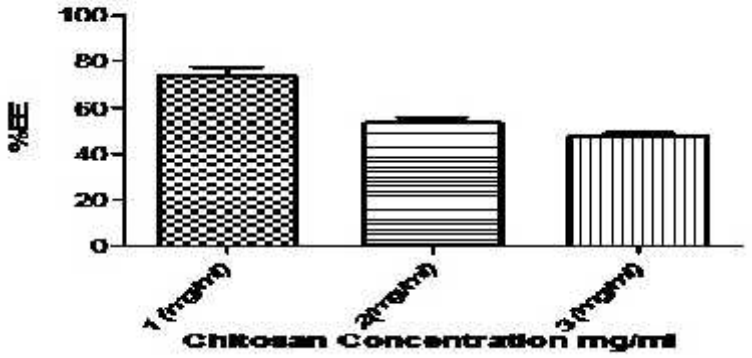

Figure.23: Bar diagram showing effect of chitosan concentration on Ketoconazole entrapment efficiency (%EE) of nano-formulations (CS1, CS2, CS3) at physiological pH and temperature. The error bar indicates the standard deviation averaged from three measurements.

4.3.3. Comparative study of cumulative *in-vitro* drug release profile of Ketoconazole

The cumulative drug release percentage of Ketoconazole from chitosan nanoparticle formulation CS1 and thiolated chitosan nanoparticles showed sustained and steady release behavior for up to 10 h and thereafter no significant release was seen (Fig 24). The CS1 formulation and thiolated chitosan nanoparticles were found to be most suitable for the Ketoconazole liberation from chitosan nanoparticles because of its sustained release profile and higher drug entrapment efficiency. The free Ketoconazole was showing a biphasic or irregular release pattern where 80% drug released in just 1 h and remaining in 10 h which could be responsible for variable availability of drug. Other oral formulation of Ketoconazole such as Nizoral associated with liver damage (Gupta et al., 2015).

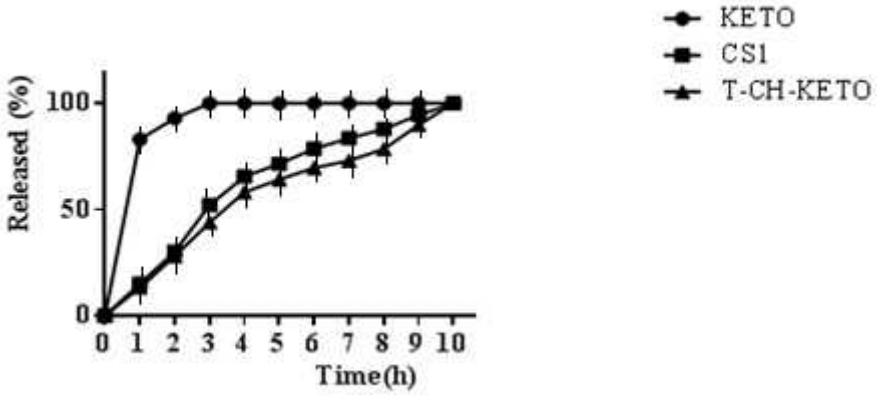

Figure.24: Cumulative drug release percentage profile of free Ketoconazole (KETO), Ketoconazole from chitosan nanoparticle (CS1) and thiolated chitosan nanoparticles (T-CH-KETO) up to 10 h at physiological pH and temperature.

4.3.4. Fourier-Transform Infra-Red Spectroscopy

The FTIR spectra of pure chitosan fig. 25 (a), chitosan nanoparticles fig. 25 (b) and Ketoconazole loaded chitosan nanoparticles (CS1) fig. 25 (c) showed. In the chitosan spectra, the strong and wide peak in the 3500-3300 area was mainly due to the O-H bonding stretching vibration. The peaks of N-H stretching from primary amine and type II amide were overlapped in the same region. The peak for asymmetric stretch of C-O-C was found at 1150 cm^{-1} and the peak at 1317 cm^{-1} belongs to the type 1 amine C-N stretching vibration. In chitosan-TPP nanoparticles the tip of the peak of 3438 cm^{-1} had a shift to 3320 cm^{-1} and peak also becomes wider with increased relative intensity indicating increased hydrogen bonding. In nanoparticles the peaks for N-H bending vibration of amine I at 1600 cm^{-1} and the amide II carbonyl stretch at 1650cm^{-1} shifted to 1540 cm^{-1} and 1630 cm^{-1}, respectively. The cross-linked chitosan also showed a P=O peak at 1170 cm^{-1} which may be attributed to the linkage of phosphoric group of TPP and ammonium ion of chitosan (Mohammadpour et al., 2012). In Ketoconazole loaded chitosan nanoparticle spectra, no changes in peaks observed as compared to chitosan nanoparticle spectra and this confirmed that the Ketoconazole was entrapped in the chitosan matrix without any kind of chemical linkage (Mohammadpour et al., 2012).

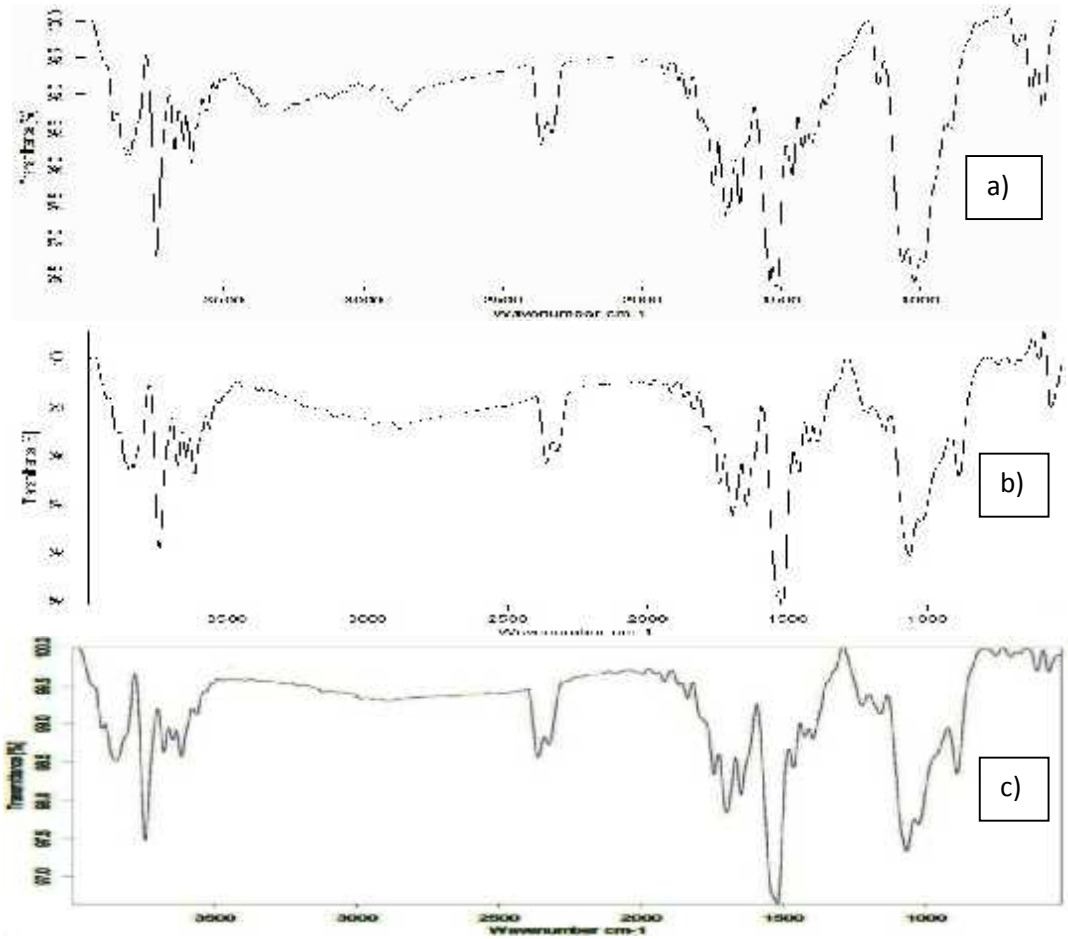

Figure.25 (a), (b), (c): FTIR analysis shows (a) chitosan, (b) chitosan-TPP nanoparticles and (c) chitosan nanoparticles loaded with Ketoconazole (CS1).

4.3.5. X-Ray Crystallography

The crystalline phase identification of Ketoconazole loaded chitosan nanoparticles (CS1) was carried out using X-ray diffraction (XRD). It is a non-destructive technique widely used for the characterization of crystalline/amorphous nature of the materials. The XRD of the chitosan fig. 26 (a), chitosan nanoparticles fig. 26 (b), pure Ketoconazole fig. 26 (c) and Ketoconazole loaded chitosan nanoparticles fig. 26 (d) were determined (Figure. 26). XRD patterns of chitosan and chitosan nanoparticles showed peaks at 2θ-scattered angles of 20 to 30; these peaks were indicating the crystalline nature of chitosan, chitosan nanoparticles. The XRD pattern of pure Ketoconazole was showing polycrystalline behavior with many sharp peaks (Fig 26c). The polycrystalline peaks of Ketoconazole disappeared and width increased in Ketoconazole loaded chitosan nanoparticle formulation (CS1) as evident in fig. 26(d) (Wang et al., 2016). This confirms that Ketoconazole present in the core of chitosan nanoparticles in amorphous state which is a characteristic feature for solubility enhancement. This pattern of XRD was also investigated by other scientists with drug Niclosamide (Naqvi et al., 2017).

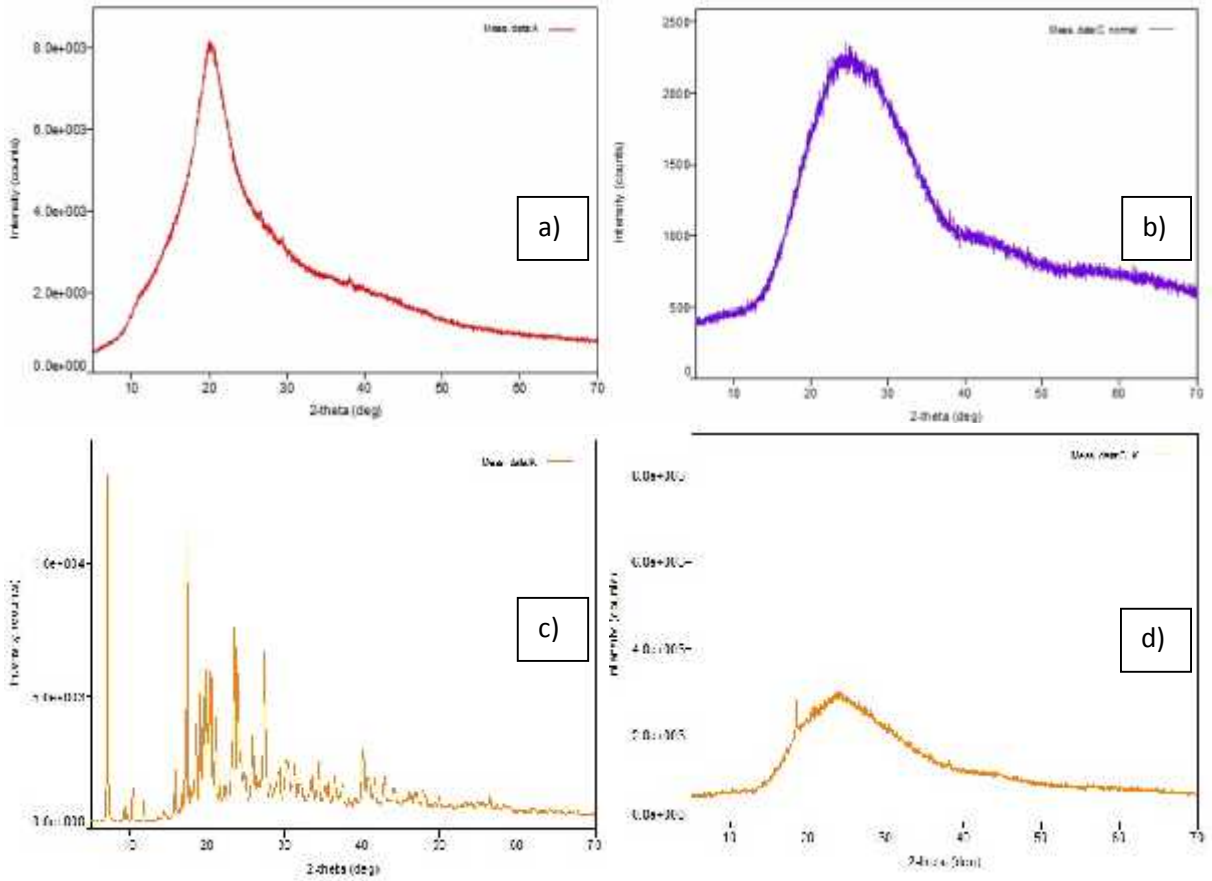

Figure.26: XRD spectra of a) pure chitosan, b) chitosan nanoparticles, c) pure Ketoconazole and d) Ketoconazole loaded chitosan nanoparticles (CS1).

4.3.6. Zeta-potential analysis of Ketoconazole loaded chitosan nanoparticles

Zeta potential value for Ketoconazole loaded chitosan nanoparticle (CS1) was found to be +29.61mV (Figure.27). Zeta potential values provide an important criterion for the stability of colloidal system. It was found that higher the zeta potential less will be the particle aggregation, due to electric repulsion and hence higher stability of nanoparticles. The higher the particles are equally charged, the greater is the electrostatic repulsion between the particles and longer is the physical stability. The positive and higher value of zeta potential indicated the positive charge on the surface of Ketoconazole loaded chitosan nanoparticles and their higher stability and this positive charge on the surface attributed to the quaternary ammonium groups of chitosan. Other scientists also obtained zeta potential ranging +22 to +55mV for stable chitosan nanoparticles (Yien et al., 2012).

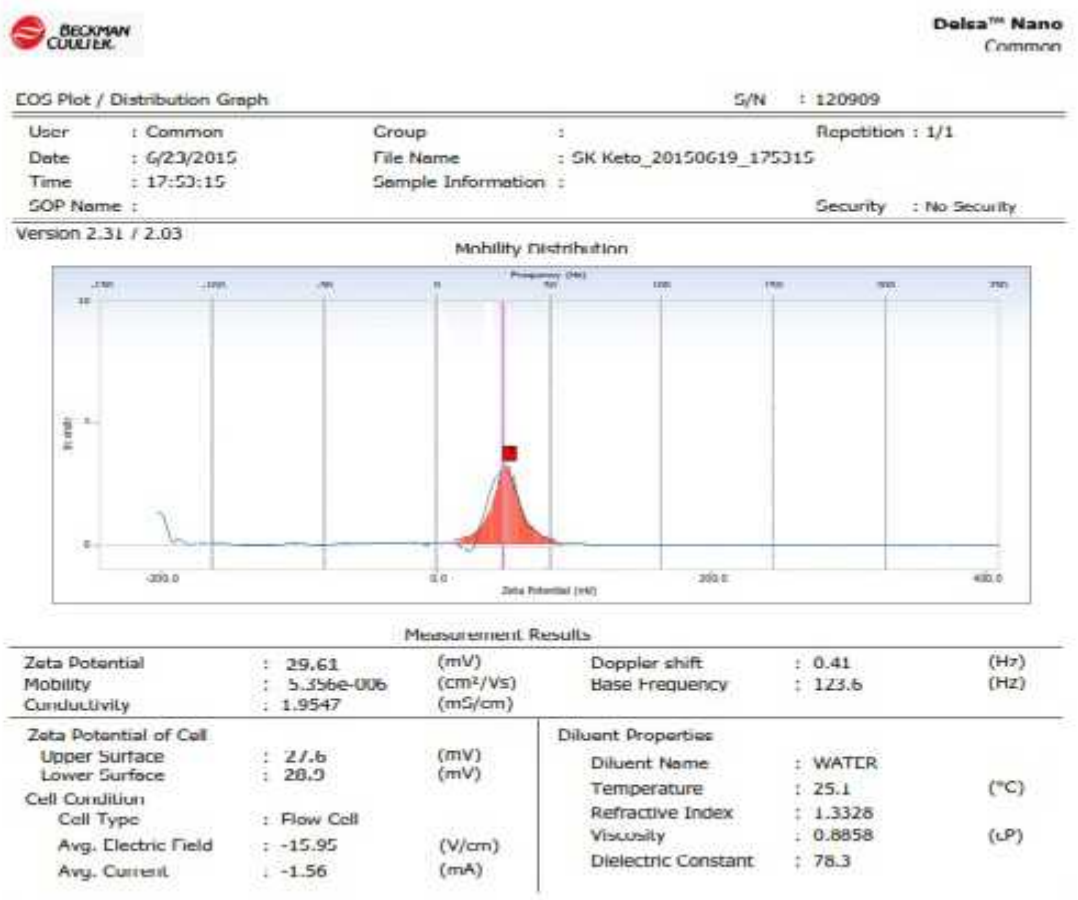

Figure.27: Zeta potential distribution plot for the Ketoconazole loaded chitosan nanoparticles (CS1).

4.3.7. Antimicrobial Study

The microbiological studies were carried out to ascertain the antifungal activity of the prepared formulation and compared with the free drug. Fig. 28 indicated that the test preparations containing the Ketoconazole loaded chitosan nanoparticles, including the free Ketoconazole demonstrated that zone of clearance (26.3mm) was seen in both the cases for up to 48 h of incubation against fungus *Coriolus versicolor* (sensitive to Ketoconazole). The commercial preparations of Ketoconazole (Nizoral) in comparison to the Ketoconazole loaded chitosan nanoparticles (CS1) exhibited nearly similar antimicrobial activity within 48 h (Kakkar et al., 2015).

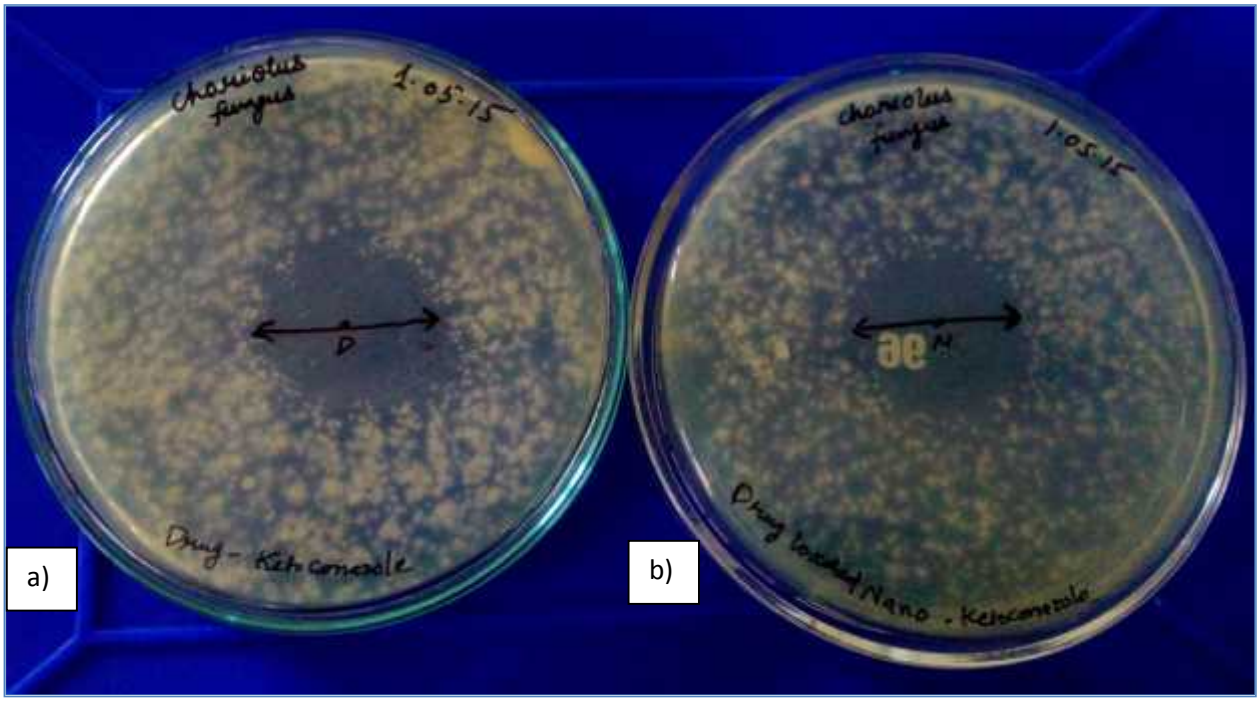

Figure.28: Zone of Clearance in the Lawn of fungus *Coriolus versicolor* by a) free drug and b) drug loaded chitosan nanoparticle after 48 h of incubation

4.4. Characterization of Ciprofloxacin loaded chitosan nanoparticles

4.4.1. Measurement of Particle size & Morphology Study

The most satisfactory nanoparticles of chitosan were obtained at a chitosan concentration of 1mg/ml in 1% acetic acid and TPP of 0.85 % (w/v) in D/W. It was obvious from the SEM study of nanoparticles that the size ranges 100-200 nm for the CS1 formulation of Ciprofloxacin and with the increase in chitosan concentration size of nanoparticles also increased. Chitosan nanoparticles loaded with Ciprofloxacin possess clear surface with uniform spherical morphology (Figure. 29). SEM images also revealed that the chitosan nanoparticles were without aggregation and the size range was found to be optimum for the oral delivery of Ciprofloxacin (Shazly et al., 2017).

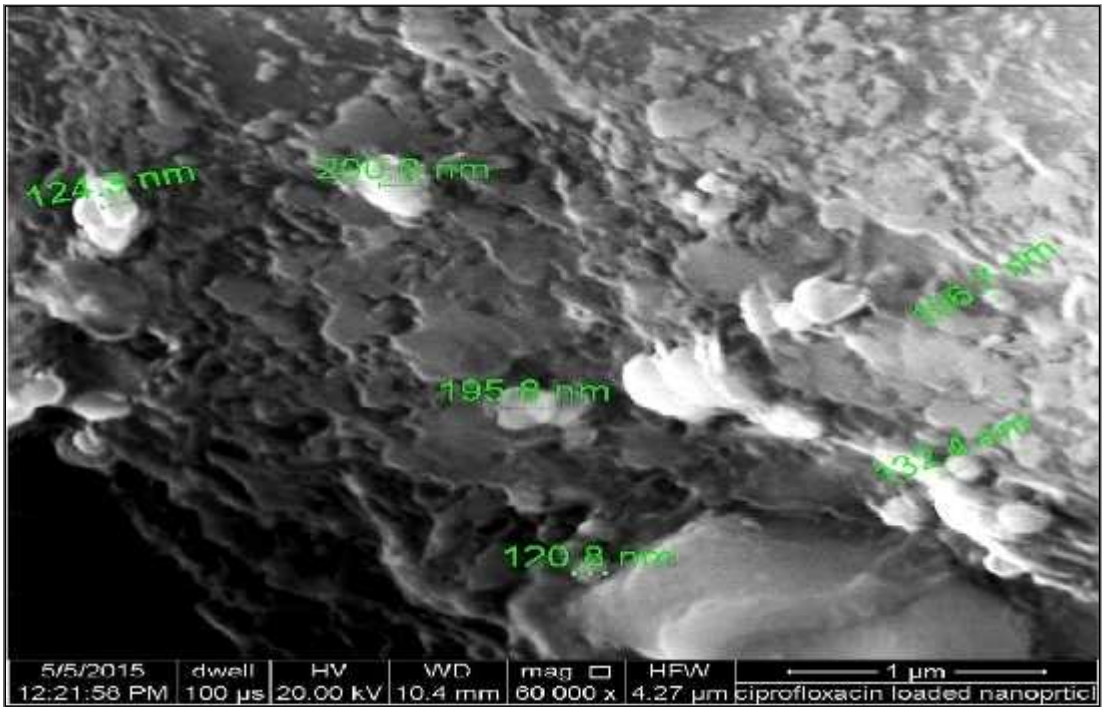

Figure.29: SEM images of chitosan nanoparticles loaded with Ciprofloxacin, a poorly soluble drug.

4.4.2. Entrapment efficiency and Percentage Yield of Ciprofloxacin loaded chitosan nanoparticle formulations

The results of entrapment efficiency revealed that drug entrapment efficiency was dependent on the polymer concentration (Fig 30). The entrapment efficiency was found to be highest for the CS1 formulation where chitosan concentration was kept minimum i.e. 1 mg/ml. With the increasing concentration of chitosan the entrapment efficiency of drug decreased due to increase in viscosity of solution. This increase of viscosity leads to hindrance in particle movement and thus decreases in particle size. Due to decrease in particle size the surface area of nanoparticles was increased which in turn resulted in higher drug entrapment efficiency. Percentage yield of 39.04 % was obtained for CS1 formulation of Ciprofloxacin.

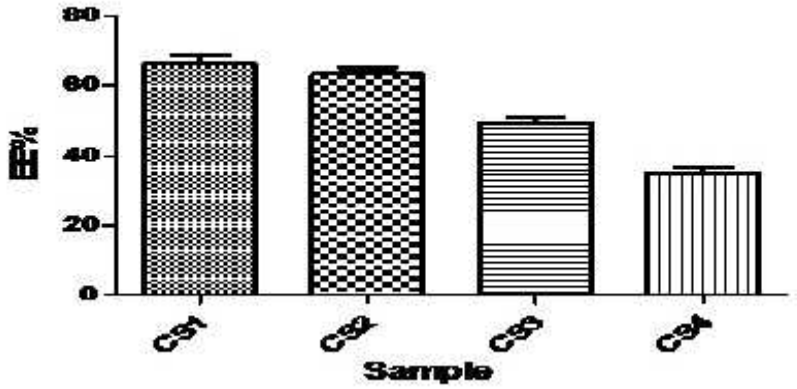

Figure.30: Bar diagram showing effect of chitosan concentration on Ciprofloxacin entrapment efficiency (%EE) of nano-formulations (CS1, CS2, CS3, CS4) at physiological pH and temperature. The error bar indicates the standard deviation averaged from three measurements.

4.4.3. Comparative study of cumulative *in-vitro* drug release profile of Ciprofloxacin

The cumulative drug release percentage of Ciprofloxacin from chitosan nanoparticle formulation CS1 and thiolated chitosan nanoparticles showed sustained and steady release behavior for up to 9 h and thereafter no significant release was noticed. The CS1 formulation and thiolated chitosan nanoparticles were found to be most suitable for the Ciprofloxacin liberation from chitosan nanoparticles because of slow and sustained release profile and higher drug entrapment efficiency. Free Ciprofloxacin was showing a biphasic or irregular release pattern where 70 % drug released in just 1 h and remaining in 9 h (Fig 31). Other extended release formulation of Ciprofloxacin found to be associated with disabling and potentially irreversible serious adverse reactions to central nervous system (US Food and Drug Administration., 2017).

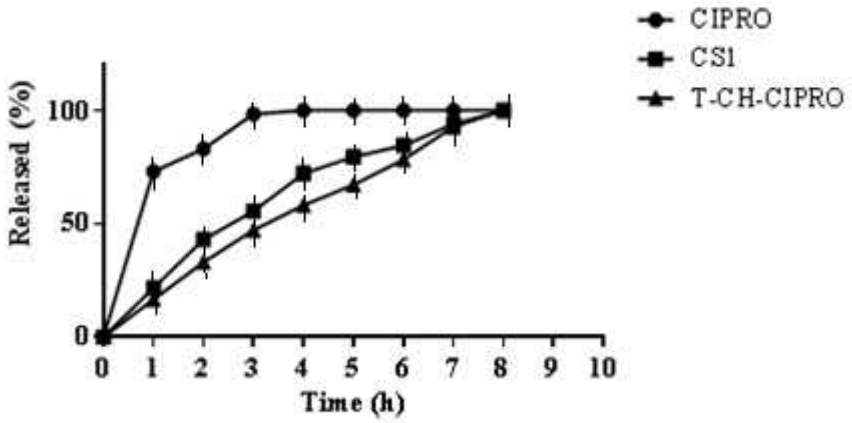

Figure.31: Cumulative drug release percentage profile of free Ciprofloxacin (CIPRO), Ciprofloxacin from chitosan nanoparticle (CS1) and thiolated chitosan nanoparticle (T-CH-CIPRO) up to 9 h at physiological pH and temperature.

4.4.4. Fourier-Transform Infra-Red Spectroscopy

The FTIR spectra of pure chitosan fig. 32 (a), chitosan nanoparticles fig. 32 (b), pure Ciprofloxacin fig. 32 (c) and Ciprofloxacin loaded chitosan nanoparticles (CS1) fig. 32 (d) showed. In the chitosan spectra, the strong and wide peak in the 3500-3300 area was mainly attributed to the O-H stretching vibration. The peaks of N-H stretching from primary amine and type II amide were overlapped in the same region. The peak for asymmetric stretch of C-O-C was at 1150 cm^{-1} and the peak at 1317 cm^{-1} belongs to the type 1 amine C-N stretching vibration. In chitosan-TPP nanoparticles the tip of the peak of 3438 cm^{-1} had a shift to 3320 cm^{-1} which becomes wider with increased relative intensity indicating increased hydrogen bonding. In nanoparticles the peaks for N-H bending vibration of amine I at 1600 cm^{-1} and the amide II carbonyl stretch at 1650cm^{-1} shifted to 1540 cm^{-1} and 1630 cm^{-1}, respectively. The cross-linked chitosan also showed a P=O peak at 1170 cm^{-1} (Fig 32) These results attributed to the linkage of phosphoric group of TPP and ammonium ion of chitosan (Mohammadpour et al., 2012). In Ciprofloxacin loaded chitosan nanoparticle spectra, no changes in peaks was observed this confirmed that the Ciprofloxacin was entrapped in the chitosan matrix without any chemical linkage (Mohammadpour et al., 2012).

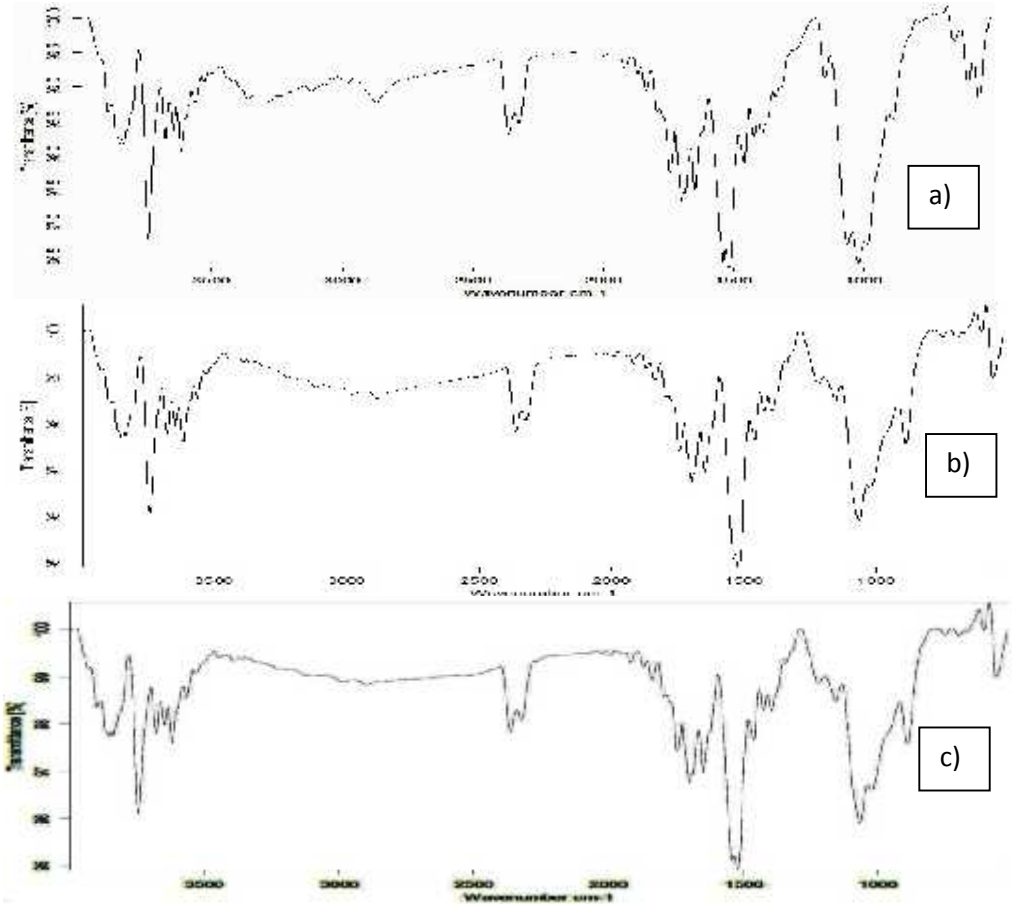

Figure.32 (a), (b), (c): FTIR analysis shows (a) chitosan, (b) chitosan-TPP nanoparticles, (c) chitosan nanoparticles loaded with Ciprofloxacin (CS1).

4.4.5. X-Ray Crystallography

The crystalline phase identification of the Ciprofloxacin loaded chitosan nanoparticle (CS1) was carried out using X-ray diffraction (XRD). It is a non-destructive technique widely used for the characterization of crystalline/amorphous nature of the materials. The XRD spectra of the chitosan fig 33(a), chitosan nanoparticles fig 33(b), pure Ciprofloxacin fig 33(c) and Ciprofloxacin containing chitosan nanoparticles (CS1) fig 33 (d) were determined (Figure. 33). XRD patterns of chitosan, chitosan nanoparticles showing sharp peaks at 2θ-scattered angles of 20 to 30. The pure Ciprofloxacin XRD pattern consisted of many sharps peaks at different angles that represent its polycrystalline behavior (Fig 33). All these peaks were indicating the crystalline nature of chitosan, chitosan nanoparticles and polycrystallanity of Ciprofloxacin. Ciprofloxacin crystalline peak disapperared and peak width increased in the Ciprofloxacin loaded chitosan nanoparticle formulation (CS1) (Fig 33) (Wang et al., 2016). This confirmed that the Ciprofloxacin present in the core of chitosan nanoparticles was in amorphous state that may be an important criterion for increased solubility. This pattern of XRD was also investigated by other scientists with drug Niclosamide (Naqvi et al., 2017).

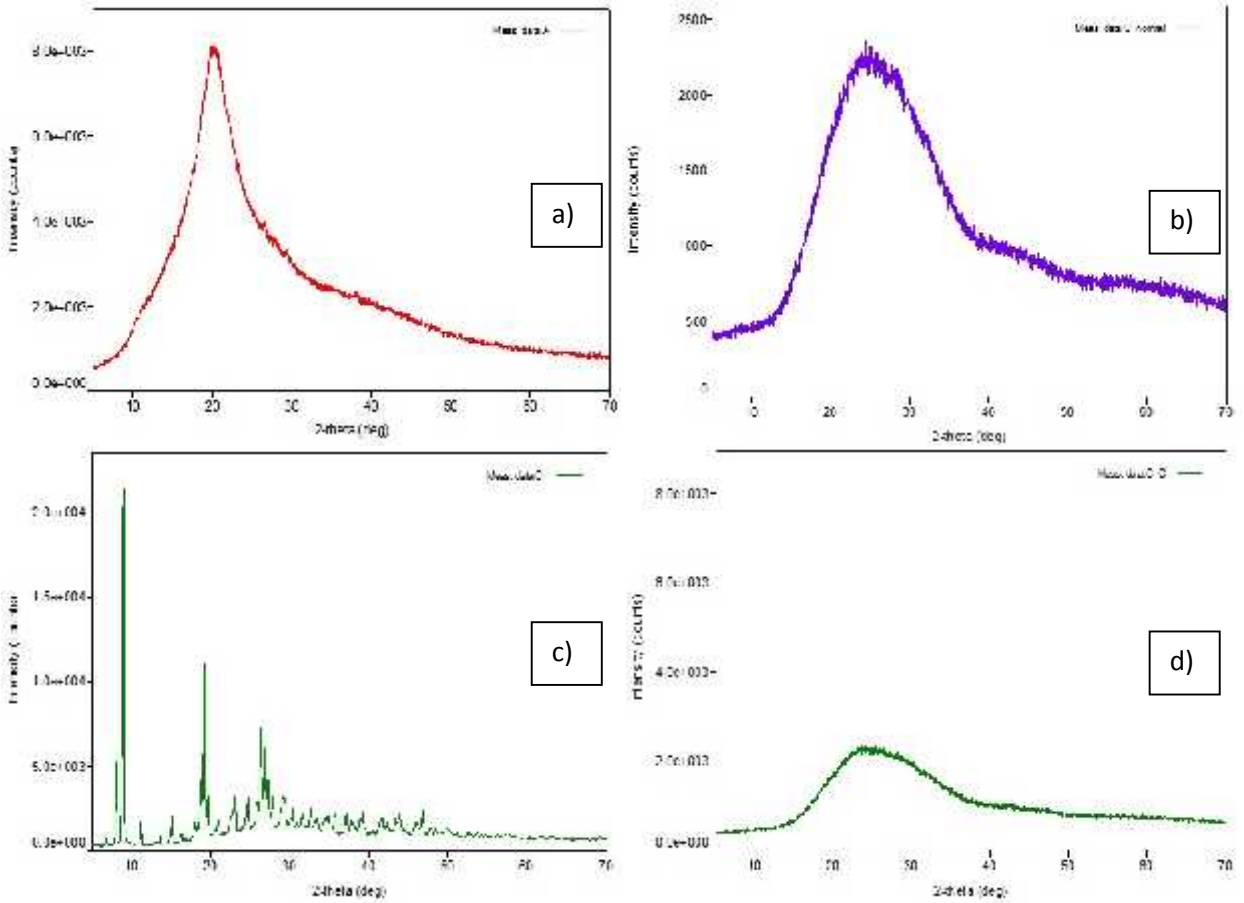

Figure.33: XRD spectra of a) pure chitosan, b) chitosan nanoparticles, c) pure Ciprofloxacin and d) Ciprofloxacin loaded chitosan nanoparticles (CS1).

4.4.6. Zeta-potential analysis of Ciprofloxacin loaded chitosan nanoparticles

Zeta potential value for the Ciprofloxacin loaded chitosan nanoparticle (CS1) was found to be +27.22 mV (Figure 34). Zeta potential values provide an important criterion for the stability of colloidal system. The higher the particles are equally charged, the greater will be the electrostatic repulsion between the particles and longer is the physical stability. This is the electric potential that exists at the shear plane of a particle, related to both the surface charge and local environment of the nanoparticle. The positive value of zeta potential indicated the positive surface of Ciprofloxacin loaded chitosan nanoparticles that lead to increase in its cellular uptake, adhesivity and cytotoxicity (Fröhlich et al., 2012). The positive charge on the surface of Ciprofloxacin loaded chitosan nanoparticle formulation CS1 was might be due to presence of unreacted NH_2 groups available on chitosan surface for attachment to other negatively charged molecule. Similar types of finding were made by Yien et al in 2012.

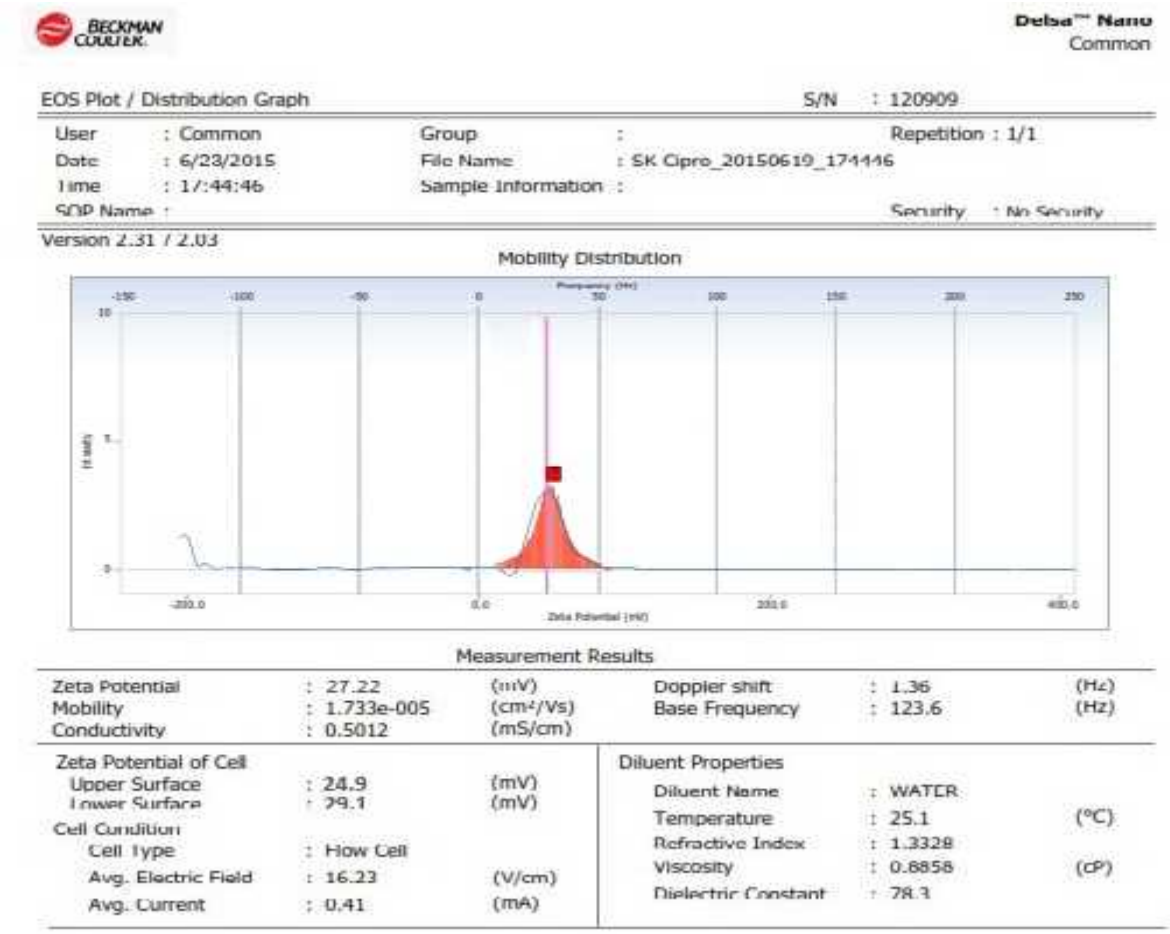

Figure.34: Zeta potential distribution plot for the Ciprofloxacin loaded chitosan nanoparticles (CS1).

4.4.7. Antimicrobial Study

The microbiological studies were carried out to ascertain the antibacterial activity of the prepared formulation and compared with the free drug. Fig. 35 indicated that both the test preparations containing the Ciprofloxacin loaded chitosan nanoparticles and the free Ciprofloxacin, demonstrated that zone of clearance (29.7 mm) was seen in both the cases for up to 48 h of incubation against *Pseudomonas aeroginosa* (highly sensitive to Ciprofloxacin). The commercial preparations of Ciprofloxacin in comparison to the Ciprofloxacin loaded chitosan nanoparticles exhibited similar antibacterial activity within 48 h (Salahuddin et al., 2016).

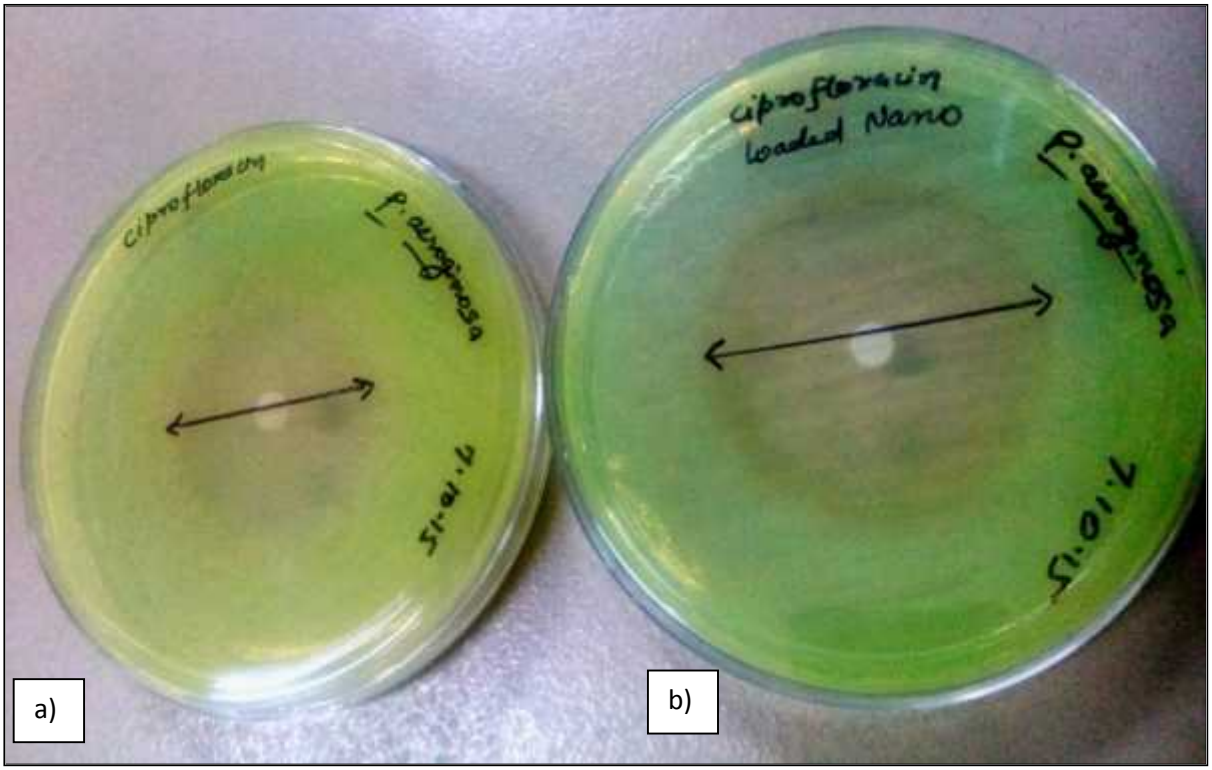

Figure.35: Zone of clearance in the lawn of *Pseudomonas aeroginosa* by a) free drug and b) drug loaded chitosan nanoparticle after 48 h of incubation.

4.5. Characterization of Vancomycin loaded chitosan nanoparticle

4.5.1. Measurement of Particle size & Morphology Study

The most satisfactory nanoparticles of chitosan were obtained at a chitosan concentration of 1mg/ml in 1% acetic acid and TPP of 0.85 % (w/v) in D/W. It was evident from the SEM study of nanoparticles that the size ranges 80-150 nm for the CS1 formulation and with the increase in chitosan concentration size of nanoparticles also increased. Vancomycin loaded chitosan nanoparticles with clear surface and uniform spherical morphology was observed (Figure 36). SEM images also revealed that the chitosan nanoparticles were without aggregation and the size range was found to be optimum for the oral delivery of Vancomycin (Xu et al., 2015).

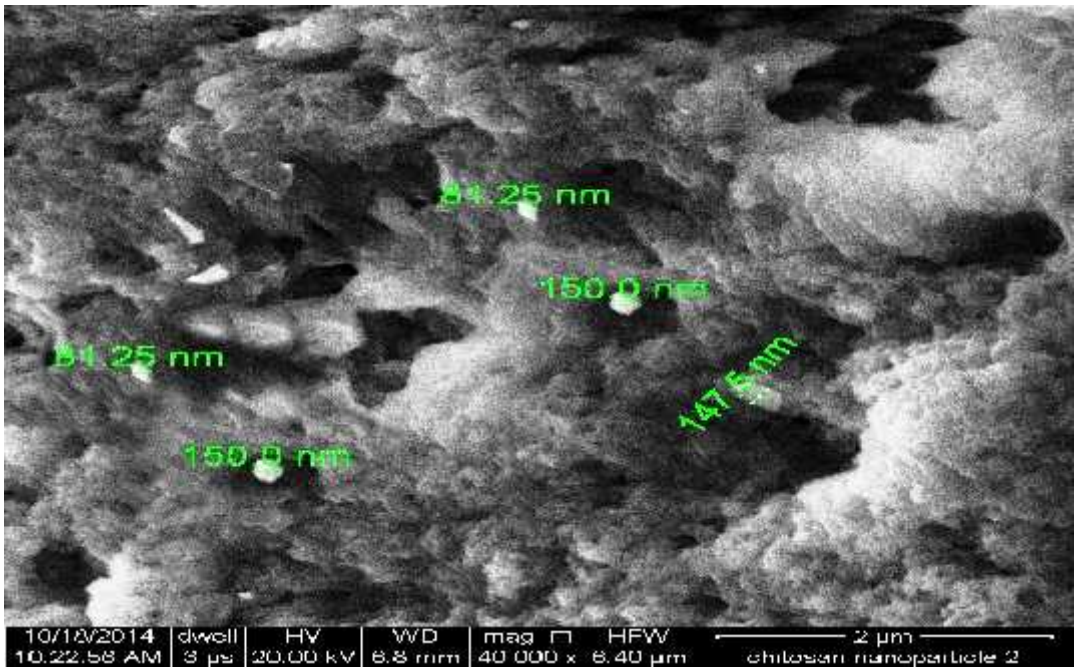

Figure.36: SEM images of chitosan nanoparticles loaded with Vancomycin, a poorly soluble drug.

4.5.2. Entrapment efficiency and Percentage Yield of Vancomycin loaded chitosan nanoparticle formulations

The results of entrapment efficiency revealed that drug entrapment efficiency was dependent on the polymer concentration. The entrapment efficiency was found to be maximum for the CS1 formulation where chitosan concentration was kept minimum i.e. 1 mg/ml. With the increasing concentration of chitosan the drug entrapment efficiency decreased due to increase in viscosity of solution that leads to hindrance in particle movement and thus decreases in particle size. Due to decrease in particle size the surface area of nanoparticles was increased which in turn results in higher drug entrapment efficiency. Percentage yield of 39.04 % was obtained for CS1 formulation of Vancomycin (Fig 37).

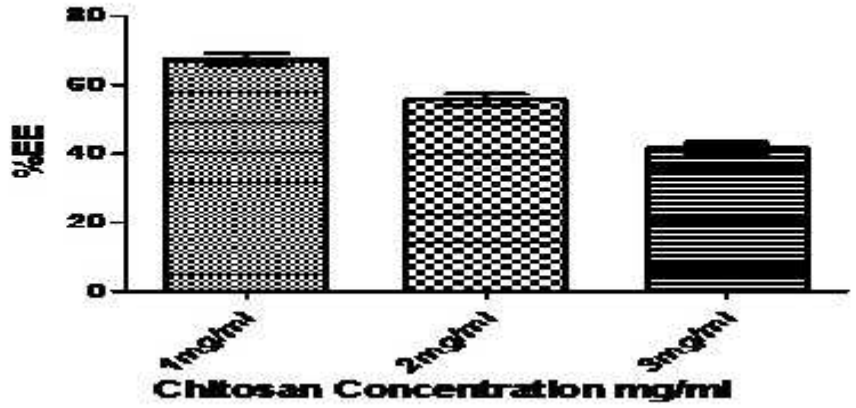

Figure.37: Bar diagram showing effect of chitosan concentration on Vancomycin entrapment efficiency (%EE) of nano-formulations (CS1, CS2, and CS3) at physiological pH and temperature. The error bar indicates the standard deviation averaged from three measurements.

4.5.3. Comparative study of cumulative *in-vitro* drug release profile of Vancomycin

The cumulative drug release percentage of Vancomycin from chitosan nanoparticle formulation CS1 and thiolated chitosan nanoparticles showed sustained and steady release behavior up to 10 h and thereafter no significant release observed (Fig 38). The CS1 formulation and thiolated chitosan nanoparticles were found to be most suitable for the Vancomycin liberation from chitosan nanoparticles because of sustained release profile and higher drug entrapment efficiency. The free Vancomycin was showing a biphasic or irregular release pattern where 70% drug released in just 1 h and remaining in 10 h. Other marketed oral formulation of Vancomycin such as Vancocin found to be associated with no major side effects (Powers et al., 2005).

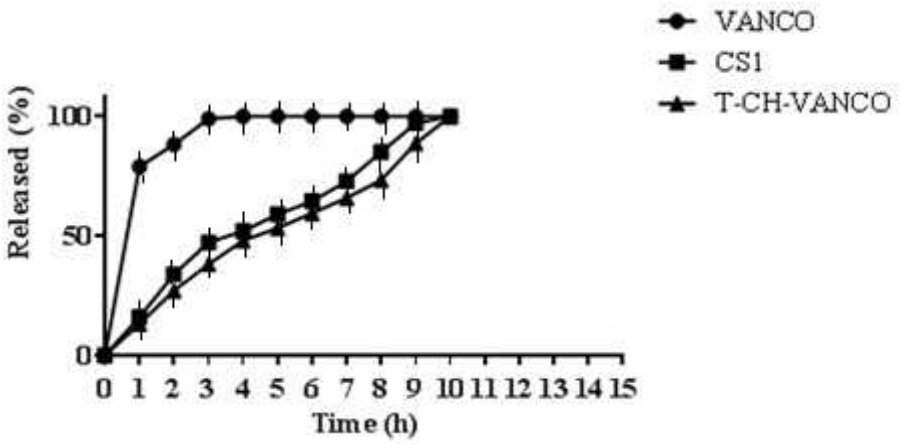

Figure.38: Cumulative drug release percentage profile of free Vancomycin (VANCO), Vancomycin from chitosan nanoparticle (CS1) and thiolated chitosan nanoparticle (T-CH-VANCO) up to 10 h at physiological pH and temperature.

4.5.4. Fourier-Transform Infra-Red Spectroscopy

In the chitosan spectra, the FTIR study showed that the strong and wide peak in the 3500-3300 range was mainly attributed to the O-H bonding stretching vibration (Fig 39 a). The peaks of N-H stretching from primary amine and type II amide were overlapped in the same region. The peak for asymmetric stretch of C-O-C was found around at 1150 cm^{-1} and the peak at 1317 cm^{-1} belongs to the type 1 amine C-N stretching vibration. In chitosan-TPP nanoparticles the tip of the peak of 3438 cm^{-1} had a shift to 3320 cm^{-1} and also becomes wider with increased relative intensity indicating increased hydrogen bonding (Fig 39 b). In nanoparticles the peaks for N-H bending vibration of amine I at 1600 cm^{-1} and the amide II carbonyl stretch at 1650cm^{-1} shifted to 1540 cm^{-1} and 1630 cm^{-1}, respectively. The cross-linked chitosan also showed a P=O peak at 1170 cm^{-1}. These results attributed to the linkage of phosphoric group of TPP and ammonium ion of chitosan (Mohammadpour et al., 2012). In Vancomycin loaded chitosan nanoparticle spectra, no changes in peaks revealed that there was no interaction between the drug and additives used in the formulation (Fig 39 c) (Mohammadpour et al., 2012).

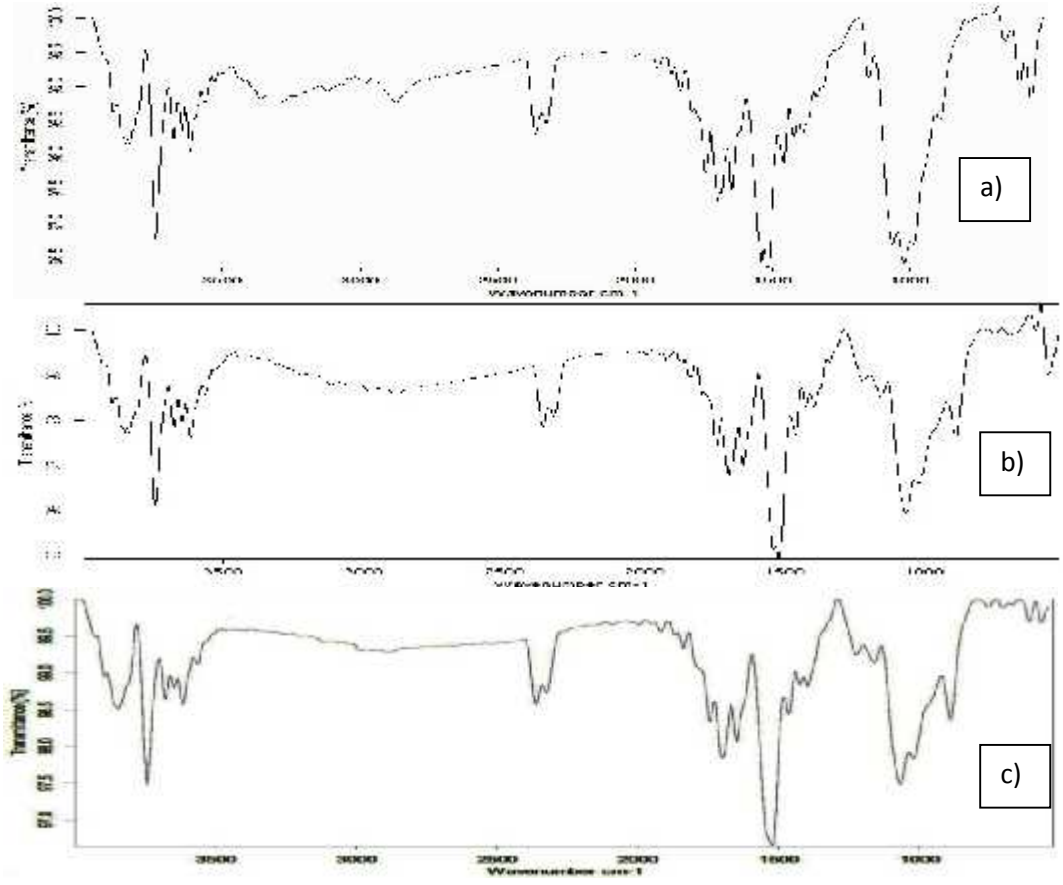

Figure.39 (a), (b), (c): FTIR analysis shows (a) chitosan, (b) chitosan-TPP nanoparticles and (c) chitosan nanoparticles loaded with Vancomycin (CS1).

4.5.5. X-Ray Crystallography

The crystalline phase identification of the studied sample (CS1) was carried out using X-ray diffraction (XRD). It is a non-destructive technique widely used for the characterization of crystalline/amorphous nature of the materials. The XRD spectra of the chitosan fig 40(a), chitosan nanoparticles fig 40(b), pure Vancomycin fig 40(c) and Vancomycin containing chitosan nanoparticles (CS1) fig 40(d) were determined (Figure. 40). XRD patterns of chitosan, chitosan nanoparticles showing no sharp peaks at 2θ-scattered angles of 20 to 30. The pure Vancomycin XRD pattern consists of single peak at 2θ-scattered angles of 20 to 40 that represented its amorphous behavior. All these peaks were indicating the non crystalline nature of chitosan, chitosan nanoparticles and Vancomycin. No peak in the Vancomycin loaded chitosan nanoparticle formulation (CS1) confirms the amorphous nature of drug loaded formulation (CS1) (Wang et al., 2016). This pattern of XRD was also investigated by other scientists with drug Niclosamide (Naqvi et al., 2017).

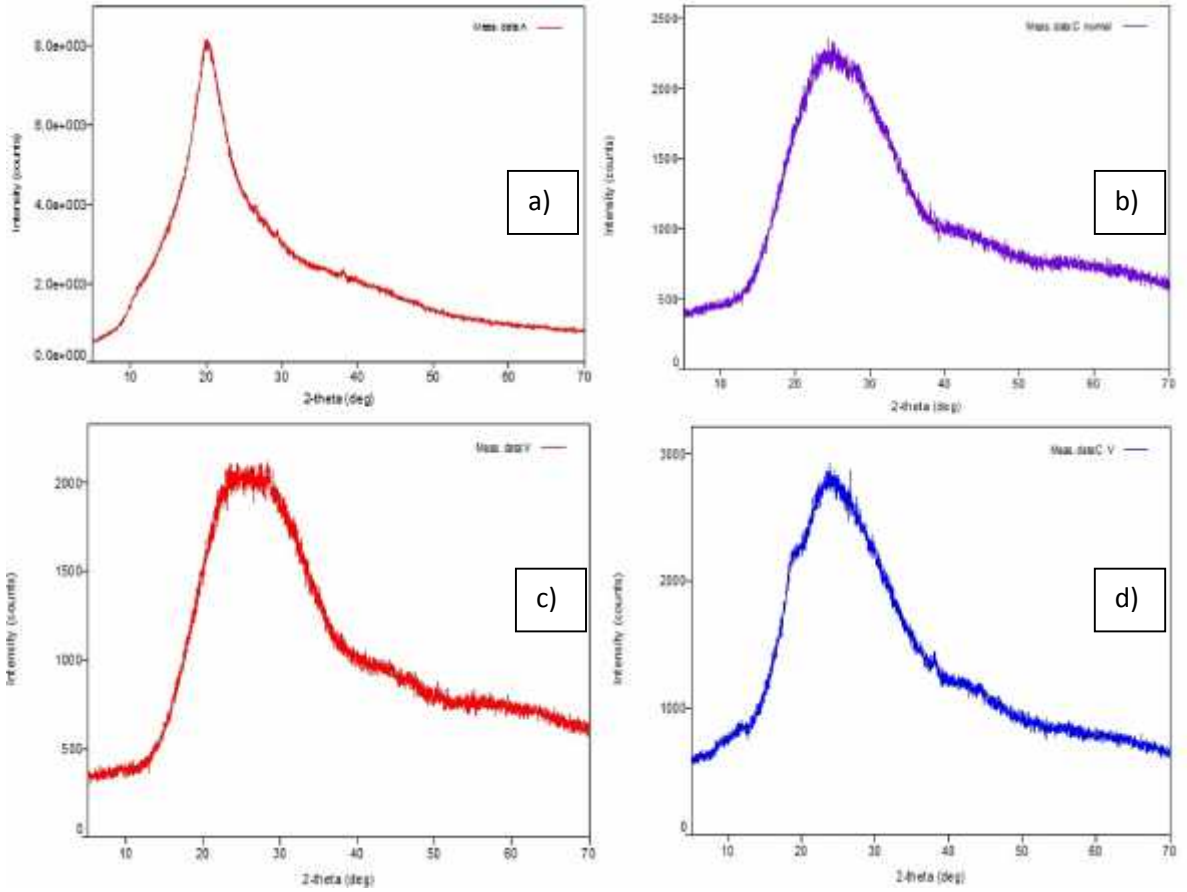

Figure.40: XRD spectra of a) pure chitosan, b) chitosan nanoparticles, c) pure Vancomycin and d) Vancomycin loaded chitosan nanoparticles (CS1).

4.5.6. Zeta-potential analysis of Vancomycin loaded chitosan nanoparticles

Zeta potential value for the Vancomycin loaded chitosan nanoparticle (CS1) was found to be +27 mV (Figure 41). Zeta potential values provide an important criterion for the stability of colloidal system. The higher the particles are equally charged, the greater is the electrostatic repulsion between the particles and longer is the physical stability. The positive and high value of zeta potential indicated the fair stability and positive surface charge of Vancomycin loaded chitosan nanoparticles lead to increase in its cellular uptake, adhesivity and cytotoxicity (Fröhlich et al., 2012). This positive charge on the surface of Vancomycin loaded chitosan nanoparticle formulation CS1 was may be due to presence of unreacted NH_2 groups available on chitosan surface for attachment to other negatively charged molecule. Other scientists also obtained zeta potential ranging +22 to +55mV for stable chitosan nanoparticles (Yien et al., 2012).

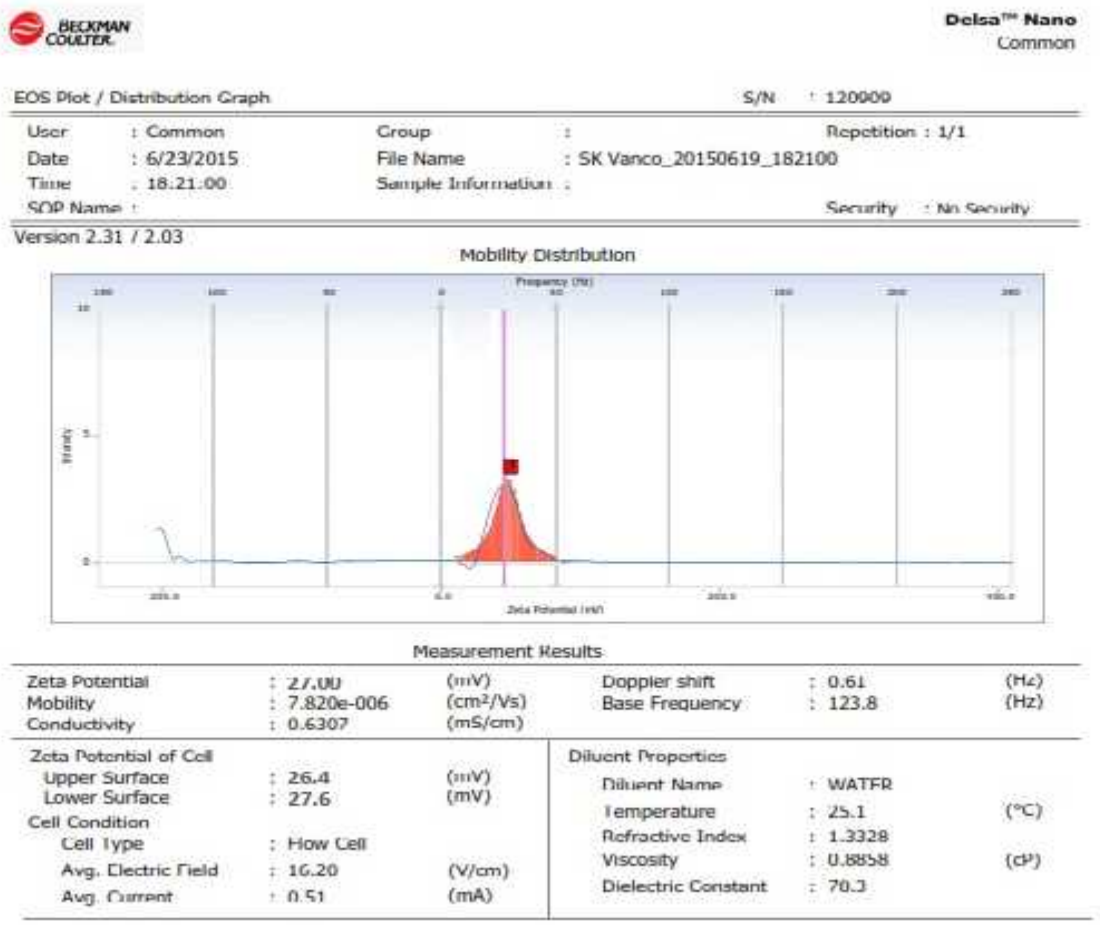

Figure.41: Zeta potential distribution plot for the Vancomycin loaded chitosan nanoparticles (CS1).

4.5.7. Antimicrobial Study

The microbiological studies were carried out to ascertain the antimicrobial/antibacterial activity of the prepared formulation and compared with the free drug. Fig. 42 indicated that the test preparations containing the Vancomycin loaded chitosan nanoparticles, including the free Vancomycin had zone of clearance of 12.2mm after 48 h of incubation against *Bacillus cereus* (sensitive to Vancomycin). The commercial preparations of Vancomycin in comparison to the Vancomycin loaded chitosan nanoparticles exhibited nearly similar antibacterial activity within 48 h (Salahuddin et al., 2016).

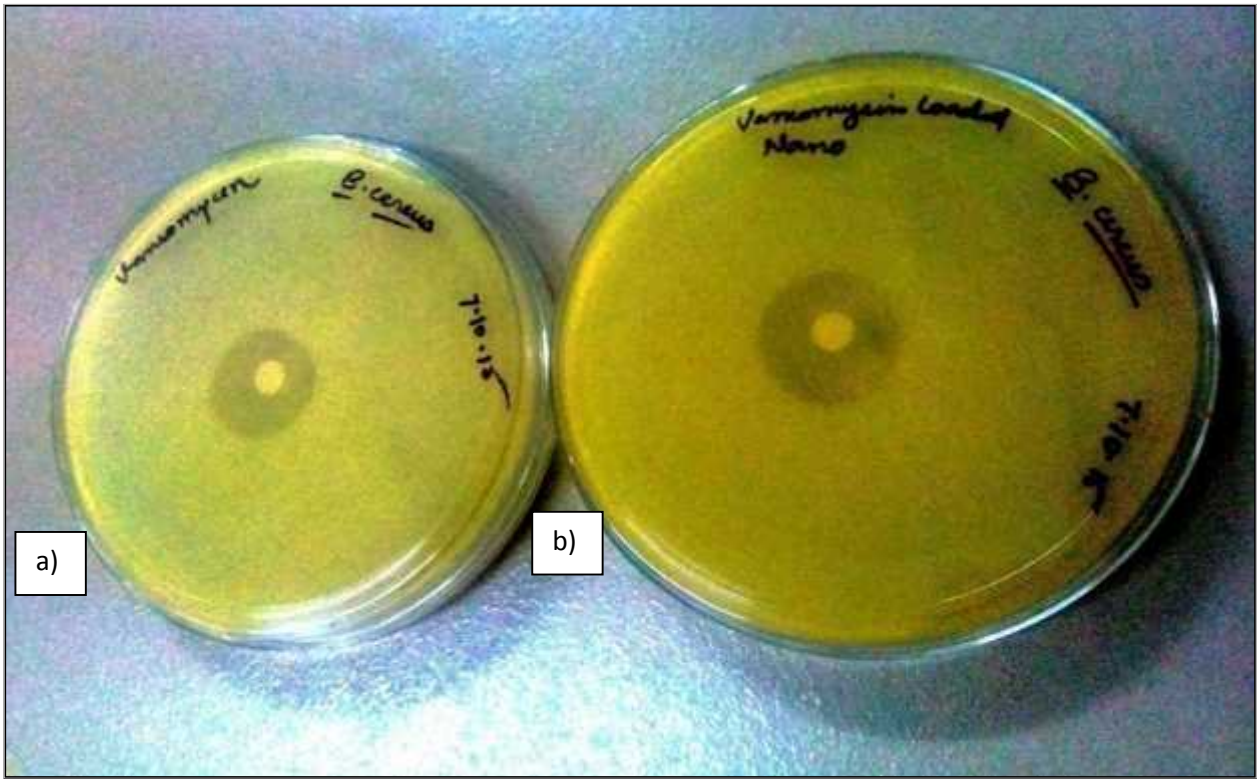

Figure.42: Zone of clearance in the lawn of *Bacillus cereus* by a) free drug and b) drug loaded chitosan nanoparticle after 48 h of incubation

4.6. Characterization of Chloramphenicol loaded chitosan nanoparticles

4.6.1. Measurement of Particle size & Morphology Study

The most satisfactory nanoparticles of chitosan were obtained at a chitosan concentration of 1mg/ml in 1% acetic acid and TPP of 0.85 % (w/v) in D/W. It was evident from the SEM study of nanoparticles that the size ranges 70-180 nm for the CS1 formulation and with the increase in chitosan concentration size of nanoparticles also increased. Further chitosan nanoparticles with clear and uniform spherical morphology were observed (Figure 43). SEM images also showed that the chitosan nanoparticles were without aggregation and the size range was found to be optimum for the oral delivery purpose of Chloramphenicol (Li et al., 2008).

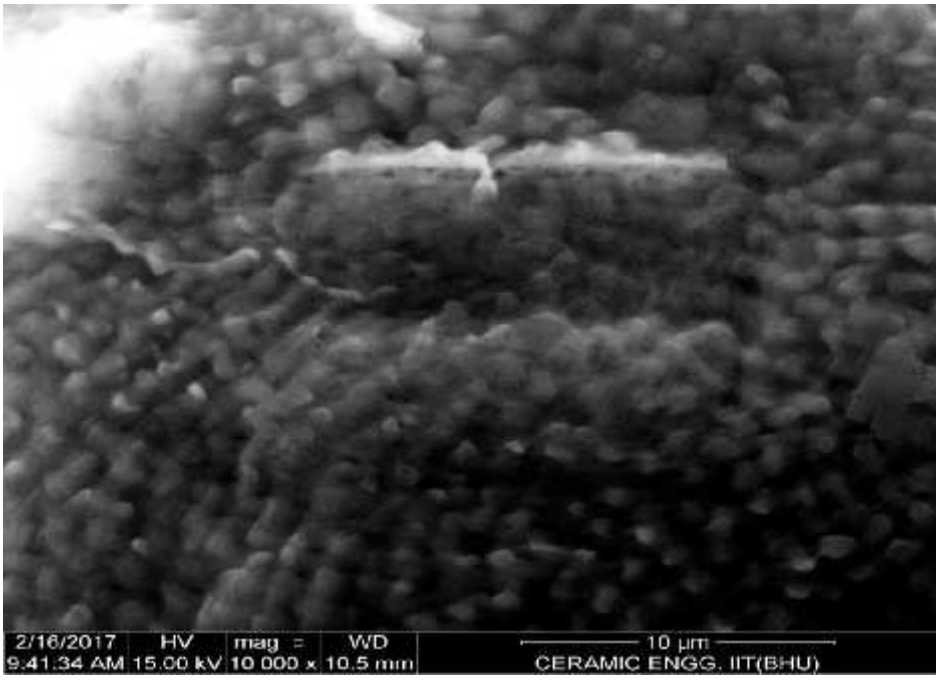

Figure.43: SEM images of chitosan nanoparticles loaded with Chloramphenicol, a poorly soluble drug.

4.6.2. Entrapment efficiency and Percentage Yield of Chloramphenicol loaded chitosan nanoparticle formulations

The entrapment efficiency was found to be maximal for the CS1 formulation where chitosan concentration was 1 mg/ml (Fig 44). With the increasing concentration of chitosan the Chloramphenicol entrapment efficiency decreases due to increase in viscosity of solution that leads to hindrance in particle movement and thus decreases in particle size. Due to decrease in particle size the surface area of nanoparticles was increased which in turn results in higher drug entrapment efficiency. Percentage yield of 39.04 % was obtained for CS1 formulation of Chloramphenicol.

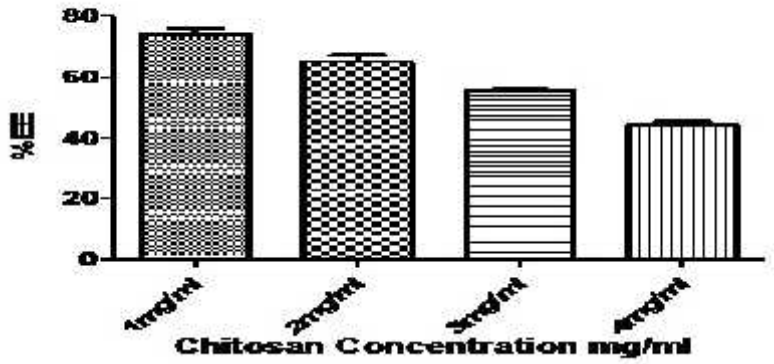

Figure.44: Bar diagram showing effect of chitosan concentration on Chloramphenicol entrapment efficiency (%EE) of nano-formulations (CS1, CS2, CS3, CS4) at physiological pH and temperature. The error bar indicates the standard deviation averaged from three measurements.

4.6.3. Comparative study of cumulative *in-vitro* drug release profile of Chloramphenicol

The cumulative drug release percentage of Chloramphenicol from chitosan nanoparticle formulation CS1 and thiolated chitosan nanoparticles showed sustained and steady release behavior up to 10 h and thereafter no significant release observed (Fig 45). The CS1 formulation and thiolated chitosan nanoparticles were found to be most suitable for the Chloramphenicol liberation from chitosan nanoparticles because of sustained release profile and higher drug entrapment efficiency whereas free Chloramphenicol was showing a biphasic and irregular release pattern where 75 % drug released in just 1h and remaining in 10 h (Fig 45). Oral formulation of Chloramphenicol such as chloramphenicol palmitate ester found to be associated with causing aplastic anemia; therefore its oral formulation was stopped in US (Dong et al., 2017).

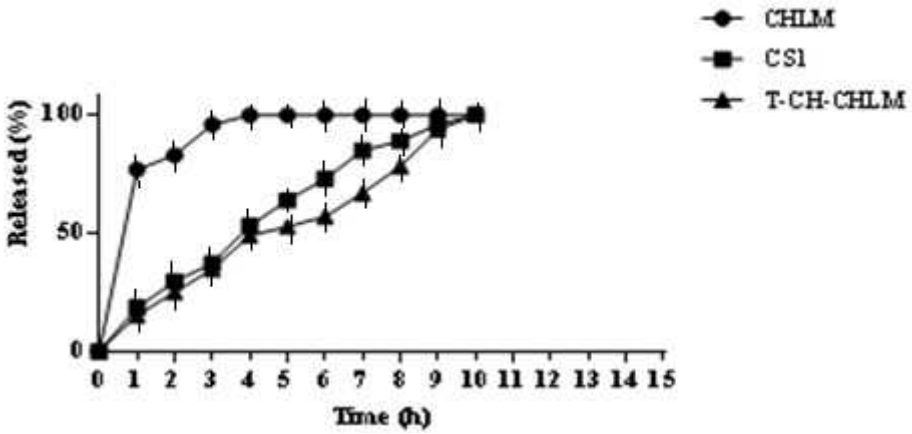

Figure.45: Cumulative drug release percentage profile free Chloramphenicol (CHLM), Chloramphenicol from chitosan nanoparticle (CS1) and thiolated chitosan nanoparticle (T-CH-CHLM) up to 10 h at physiological pH and temperature.

4.6.4. Fourier-Transform Infra-Red Spectroscopy

The FTIR spectra of pure chitosan fig 46 (a), chitosan nanoparticles fig 46 (b) and Chloramphenicol loaded chitosan nanoparticles (CS1) fig 46 (c) showed. In the chitosan spectra, the strong and wide peak in the 3500-3300 area was mainly attributed to the O-H stretching vibration. The peaks of N-H stretching from primary amine and type II amide were overlapped in the same region. The peak for asymmetric stretch of C-O-C was found around at 1150 cm^{-1} and the peak at 1317 cm^{-1} belongs to the type 1 amine C-N stretching vibration. In chitosan-TPP nanoparticles the tip of the peak of 3438 cm^{-1} had a shift to 3320 cm^{-1} and also becomes wider with increased relative intensity indicating increased hydrogen bonding. In nanoparticles the peaks for N-H bending vibration of amine I at 1600 cm^{-1} and the amide II carbonyl stretch at 1650cm^{-1} shifted to 1540 cm^{-1} and 1630 cm^{-1}, respectively. The cross-linked chitosan also showed a P=O peak at 1170 cm^{-1}. These results attributed to the linkage of phosphoric group of TPP and ammonium ion of chitosan (Mohammadpour et al., 2012). In Chloramphenicol loaded chitosan nanoparticle spectra, no changes in peaks observed that confirmed that the drug was entrapped in the chitosan matrix without any chemical linkage (Mohammadpour et al., 2012).

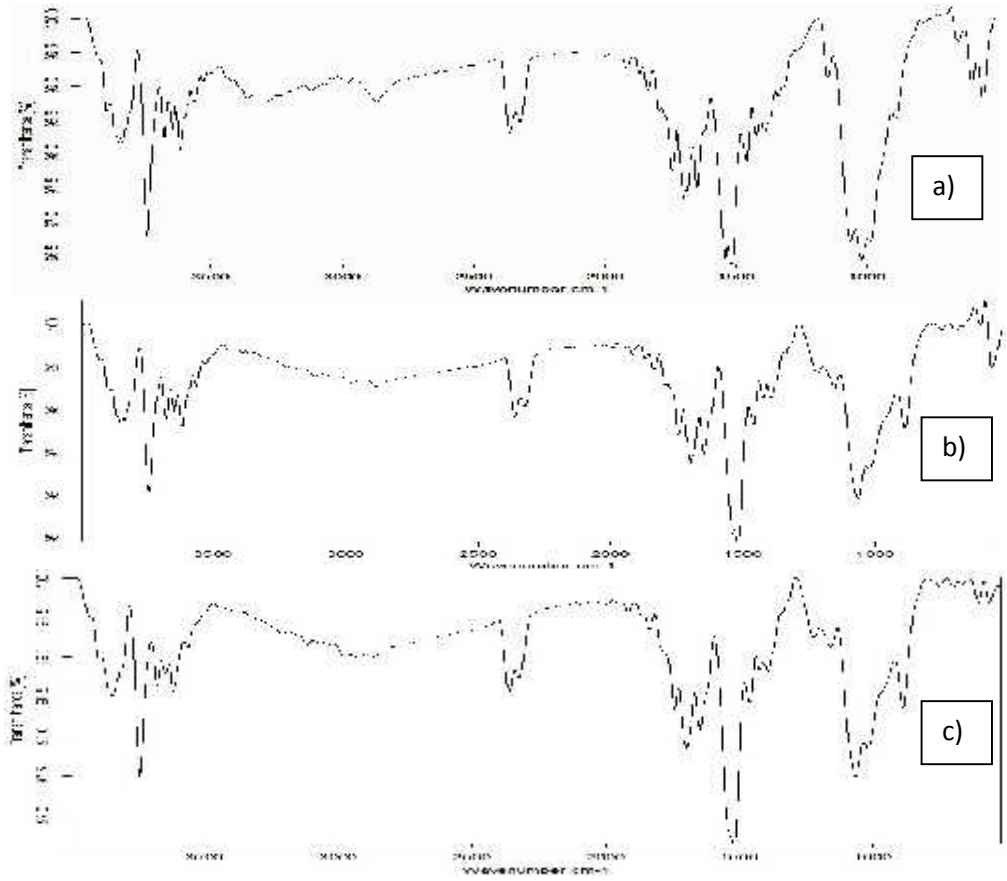

Figure.46 (a), (b), (c): FTIR analysis shows (a) chitosan, (b) chitosan-TPP nanoparticles and (c) chitosan nanoparticles loaded with Chloramphenicol (CS1).

4.6.5. X-Ray Crystallography

The crystalline phase identification of the Chloramphenicol loaded chitosan nanoparticle (CS1) was carried out using X-ray diffraction (XRD). It is a non-destructive technique widely used for the characterization of crystalline/amorphous nature of the materials. The XRD of the chitosan fig 47 (a), chitosan nanoparticles fig 47 (b), pure Chloramphenicol fig 47 (c) and Chloramphenicol containing chitosan nanoparticles fig 47 (d) were determined (Figure. 47). XRD patterns of chitosan, chitosan nanoparticles and pure Chloramphenicol showed very sharp peaks at 2θ-scattered angles of 20 to 30; these peaks were indicating the crystalline nature of chitosan, chitosan nanoparticles and Chloramphenicol. The Chloramphenicol crystalline peak disappeared in the Chloramphenicol loaded chitosan nanoparticle formulation (CS1) (Wang et al., 2016). This confirmed that the Chloramphenicol present in the chitosan nanoparticles was in amorphous state that leads to its increased solubility. This pattern of XRD was also investigated by other scientists with drug Niclosamide (Naqvi et al., 2017).

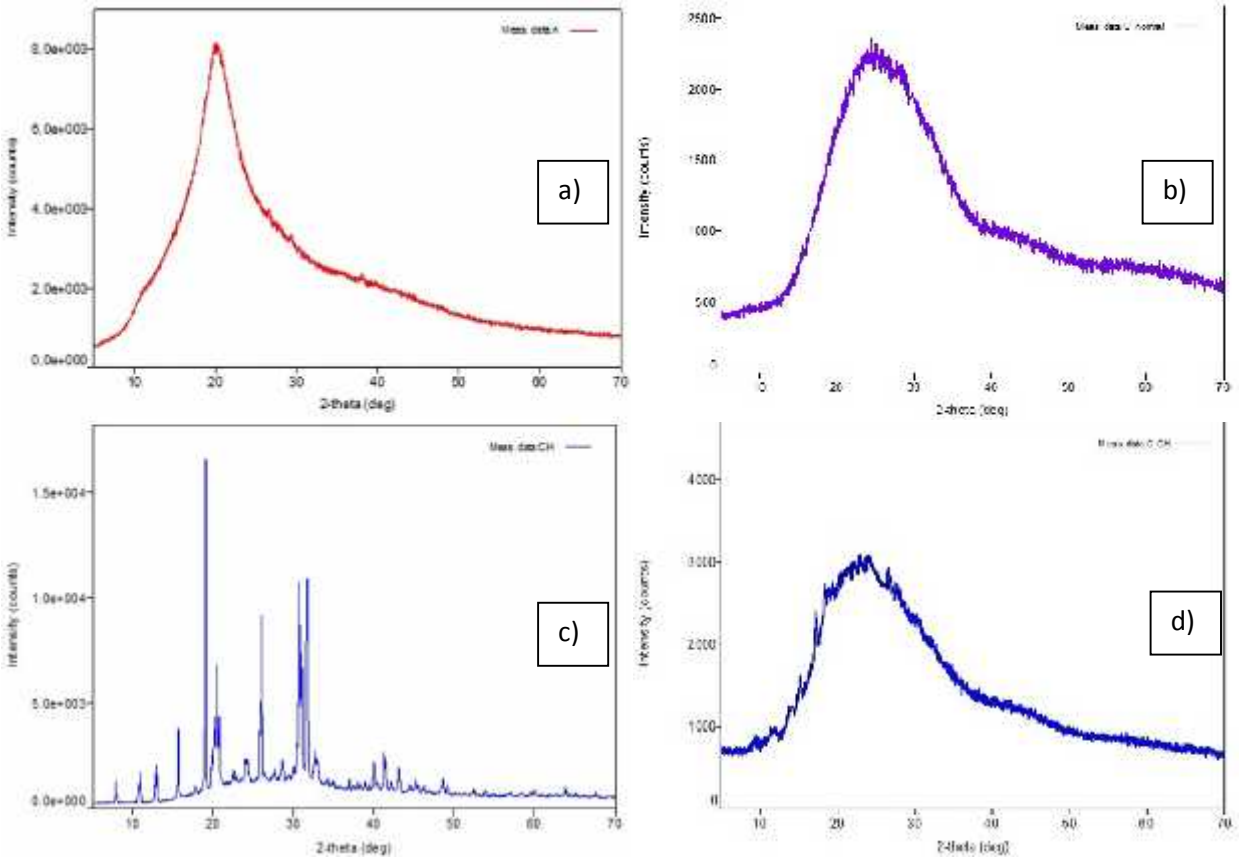

Figure.47: XRD spectra of a) pure chitosan, b) chitosan nanoparticles, c) pure Chloramphenicol and d) Chloramphenicol loaded chitosan nanoparticles (CS1).

4.6.6. Zeta-potential analysis of Chloramphenicol loaded chitosan nanoparticles

Zeta potential value for the Chloramphenicol loaded chitosan nanoparticle (CS1) was found to be +25.57mV (Figure 48). The positive & high value of zeta potential indicated the stability of Chloramphenicol loaded chitosan nanoparticles and it also increases cellular uptake of nanoparticles (Fröhlich et al., 2012). This positive charge on the surface of Chloramphenicol loaded chitosan nanoparticle formulation CS1 is may be due to presence of unreacted NH_2 groups available on chitosan surface for attachment to other negatively charged molecule. Other scientists also obtained zeta potential ranging +22 to +55mV for stable chitosan nanoparticles (Yien et al., 2012).

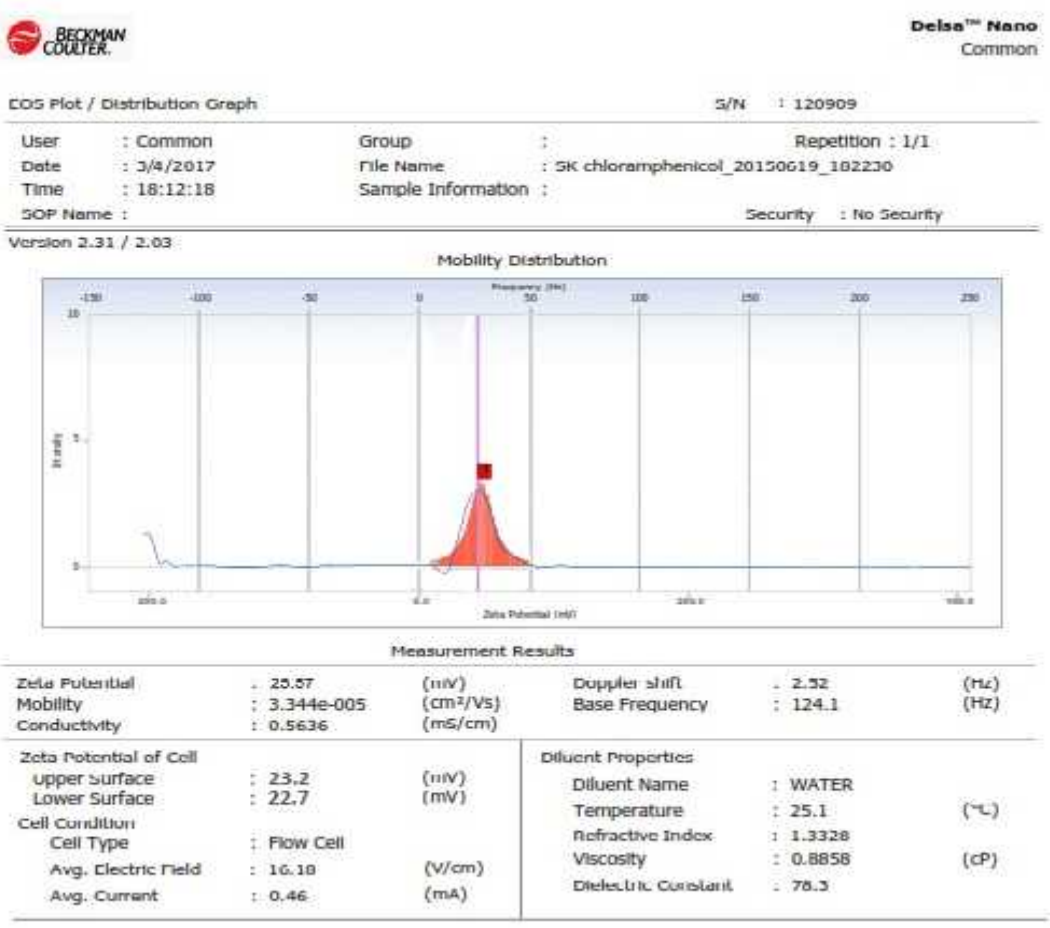

Figure.48: Zeta potential distribution plot for the Chloramphenicol loaded chitosan nanoparticles (CS1).

4.6.7. Antimicrobial Study

The microbiological studies were carried out to ascertain the antibacterial activity of the prepared formulation and compared with the free Chloramphenicol (wide spectrum antibiotic). Fig. 49 indicated that the test preparations containing the Chloramphenicol loaded chitosan nanoparticles and the free Chloramphenicol demonstrated that zone of clearance was seen in both the cases for up to 48 h of incubation against Gram Positive- *Streptococcus thermophilus (22mm)*and Gram Negative- *E.coli (21mm)*. The commercial preparations of Chloramphenicol in comparison to the Chloramphenicol loaded chitosan nanoparticles exhibited similar antibacterial activity within 48 h (Salahuddin et al., 2016).

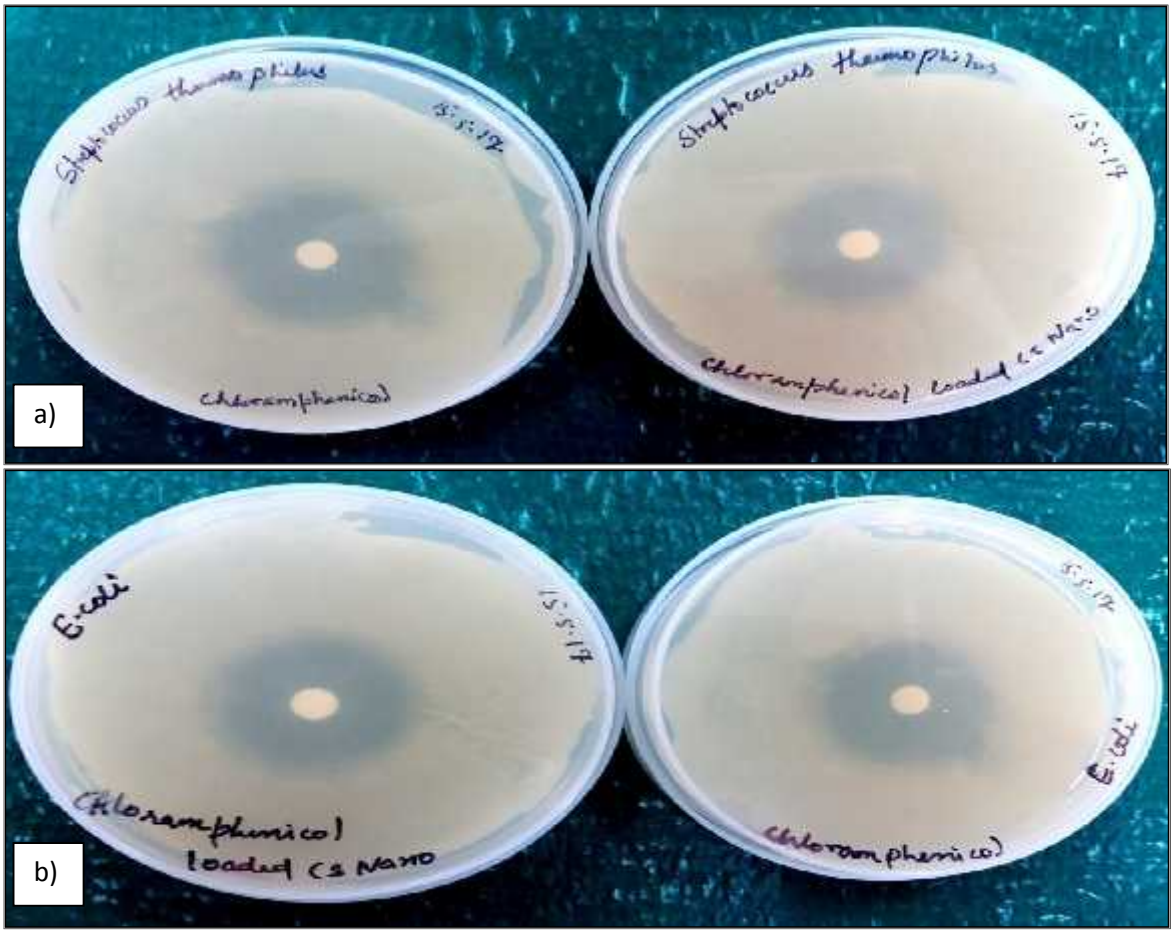

Figure.49: Zone of clearance in the lawn of a) *Streptococcus thermophilus* and b) *E.coli* by free drug and drug loaded chitosan nanoparticle after 48 h of incubation.

4.7. Kinetic Modeling of poorly soluble drug release from chitosan nanoparticles.

Mathematical models play a vital role in the interpretation of mechanism of drug release from a dosage form or formulation. It is an important tool to understand the drug release kinetics of a dosage form. Kinetic models describe the amount of drug dissolved (C) from solid dosage form as a function of test time "t" or C=f (t). Some analytical definitions of the C (t) are commonly used function, like Zero-order, First-order, Hixson–Crowell, Higuchi, Korsmeyer–Peppas etc. The mathematical model equation can be used to design new systems by selecting the optimal geometry, method of formulation and size and also aid in predicting the drug release rates and diffusion behavior from these systems by the solution of an appropriate model. Kinetic models for Amphotericin B, Ketoconazole, Ciprofloxacin, Vancomycin & Chloramphenicol release from CS1 formulation were studied.

4.7.1. Kinetic Models for Amphotericin B loaded chitosan nanoparticle formulation (CS1).

Table.15: External Factors Evaluation (EFE) matrix analysis for Amphotericin B loaded CS1.

Model Name	Amphotericin B loaded CS1		
	R^2	Slope	Intercept
Zero-order model	**0.990**	12.97	3.3
First-order model	0.915	-0.099	2.065
Higuchi model	0.860	30.48	-11.83
Korsmeyer -Peppas model	0.805	1.65	0.615
Hixson-Crowell model	0.946	0.286	-0.147

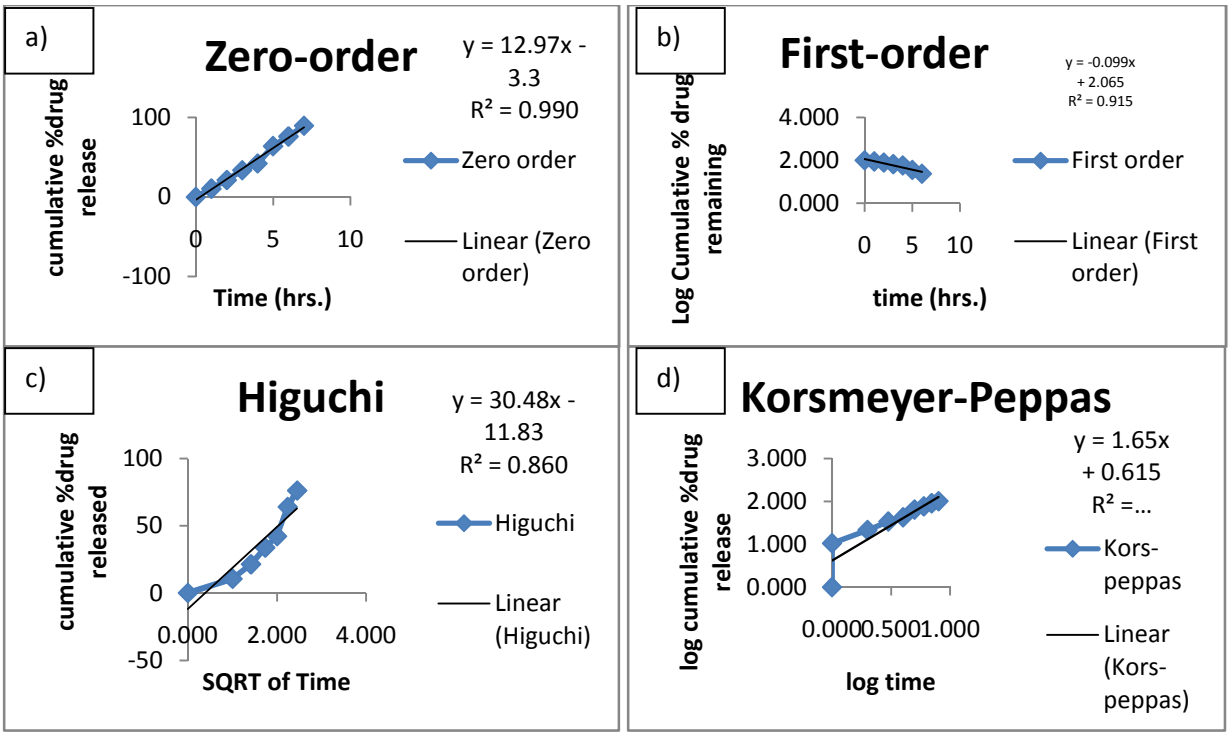

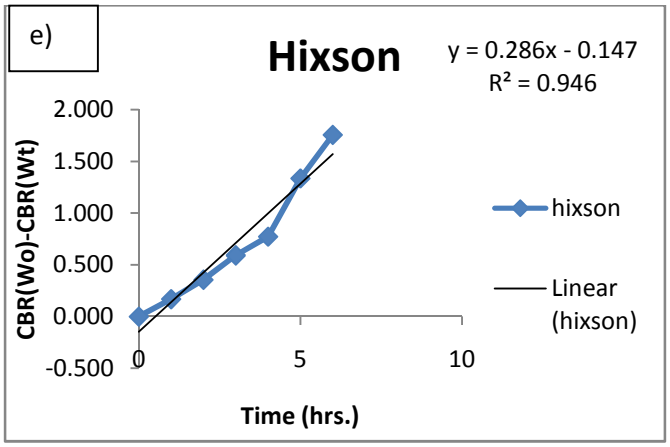

Figure.50: a) Zero-order, b) First-order, c) Higuchi, d) Korsmeyer-Peppas & e) Hixson-Crowell Model for Amphotericin B release from Chitosan nanoparticle formulation CS1.

4.7.2. Kinetic Models for free Amphotericin B release.

Table.16: External Factors Evaluation (EFE) matrix analysis for free Amphotericin B.

	Free Amphotericin B		
Model Name	**R^2**	**Slope**	**Intercept**
Zero-order model	0.661	13.51	36.68
First-order model	**0.912**	-0.365	1.921
Higuchi model	0.898	40.47	14.59
Korsmeyer-Peppas model	0.626	89.20	40.81
Hixson-Crowell model	0.908	0.813	0.399

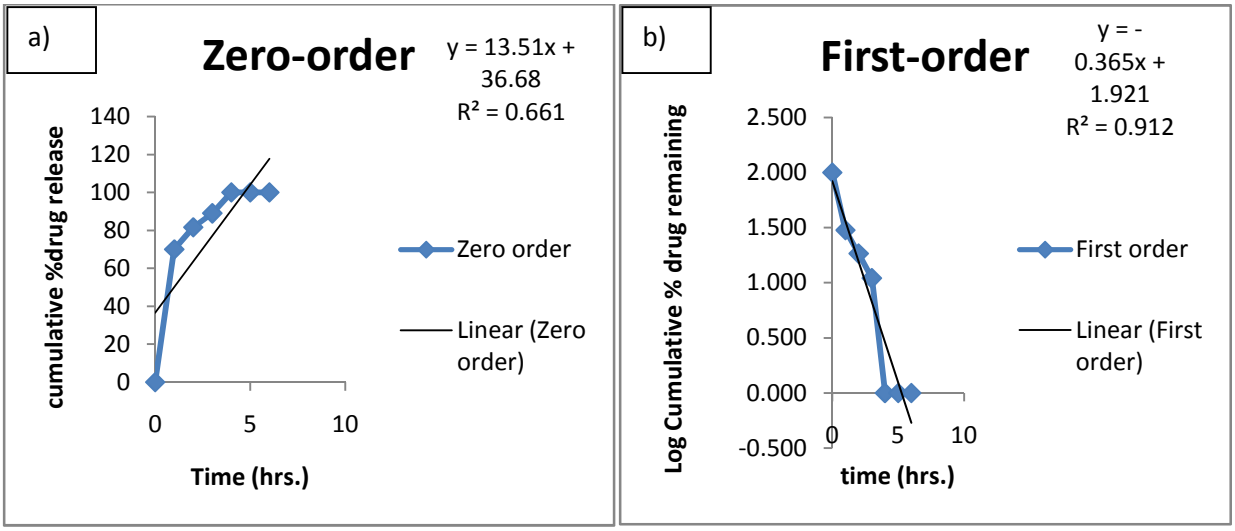

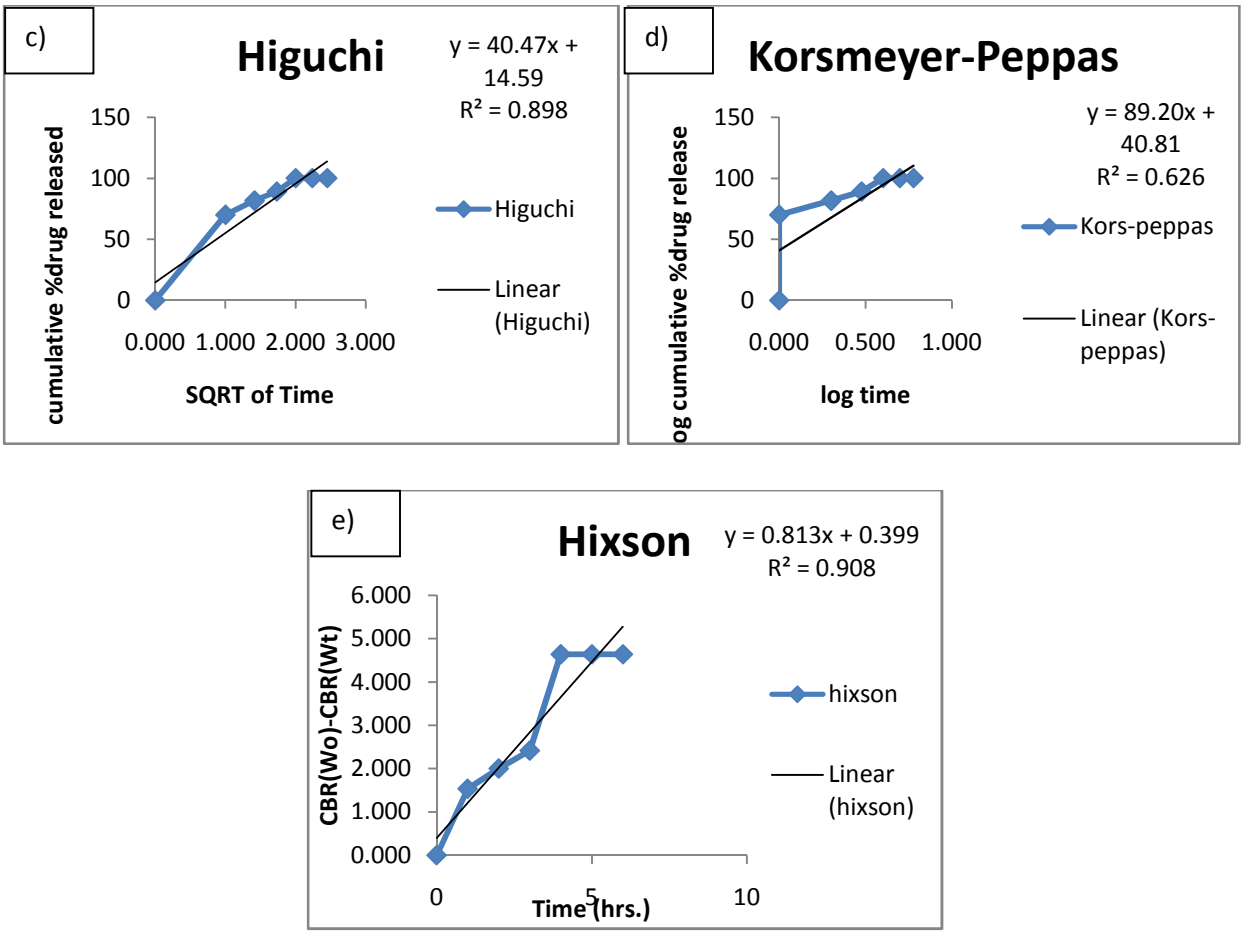

Figure.51: a) Zero-order, b) First-order, c) Higuchi, d) Korsmeyer-Peppas & e) Hixson-Crowell Model for free Amphotericin B.

The kinetic model plots obtained from the cumulative release data of Amphotericin B from chitosan nanoparticles (Fig 50), it was observed that $\mathbf{R^2}$ (coefficient of correlation) value found to be highest for zero-order model (Table.15). Amphotericin B release from chitosan nanoparticles CS1 formulation was best fitted with zero-order kinetic model. Other models like Higuchi, Kors-Peppas and Hixon used to study the release of water soluble drugs from semi solid matrix, release of drug from swelling as well as non swelling polymeric systems and drug release from systems where there is a change in surface area and diameter of particles respectively (Chime et al., 2013). The values of correlation coefficient of Korsmeyer-Peppas model for the obtained release data was low (0.805). As mentioned, release exponent of Korsmeyer-Peppas kinetic model describes Amphotericin B release mechanism and depending on its value, release process can be driven by Fickian diffusion (n equal to 0.5), polymeric matrix erosion or the combination of both mechanisms. In Higuchi model, drug releases as a diffusion process based on the Fick's law, square root time dependent. The low correlation coefficient value (0.860) described that the drug was not water soluble. In the case of free Amphotericin B release (Fig 51), the regression coefficient was highest for first-order model.

4.7.3. Kinetic Models for Ketoconazole loaded chitosan nanoparticle formulation (CS1).

Table.17: External Factors Evaluation (EFE) matrix analysis for Ketoconazole loaded CS1.

Model Name	Ketoconazole loaded CS1		
	R^2	Slope	Intercept
Zero-order model	0.967	13.73	3.56
First-order model	**0.989**	-0.116	2.032
Higuchi model	0.938	34.75	-9.024
Korsmeyer-Peppas model	0.705	1.372	0.798
Hixson-Crowell model	0.986	0.327	-0.034

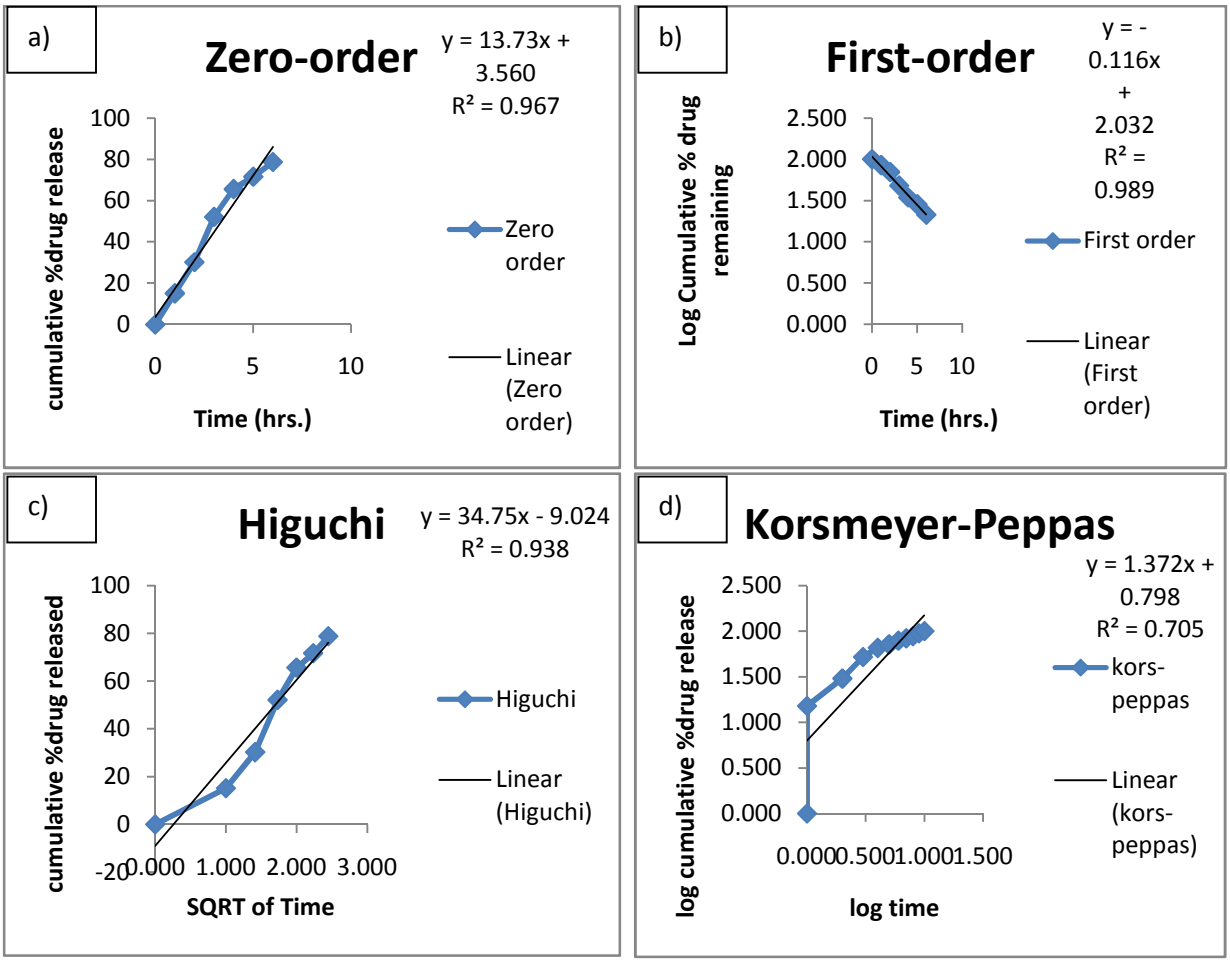

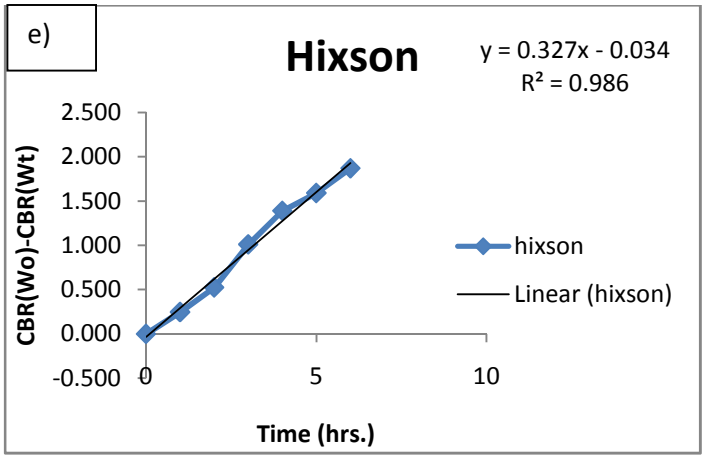

Figure.52: a) Zero-order, b) First-order, c) Higuchi, d) Korsmeyer-Peppas & e) Hixson-Crowell Model for Ketoconazole release from Chitosan nanoparticle formulation CS1.

4.7.4. Kinetic Models for free Ketoconazole release.

Table.18: External Factors Evaluation (EFE) matrix analysis for free Ketoconazole.

	Free Ketoconazole		
Model Name	**R^2**	**Slope**	**Intercept**
Zero-order model	0.51	12.17	45.75
First-order model	**0.802**	-0.332	1.579
Higuchi model	0.788	38.92	22.05
Korsmeyer -Peppas model	0.475	79.72	49.74
Hixson-Crowell model	0.789	0.749	1.09

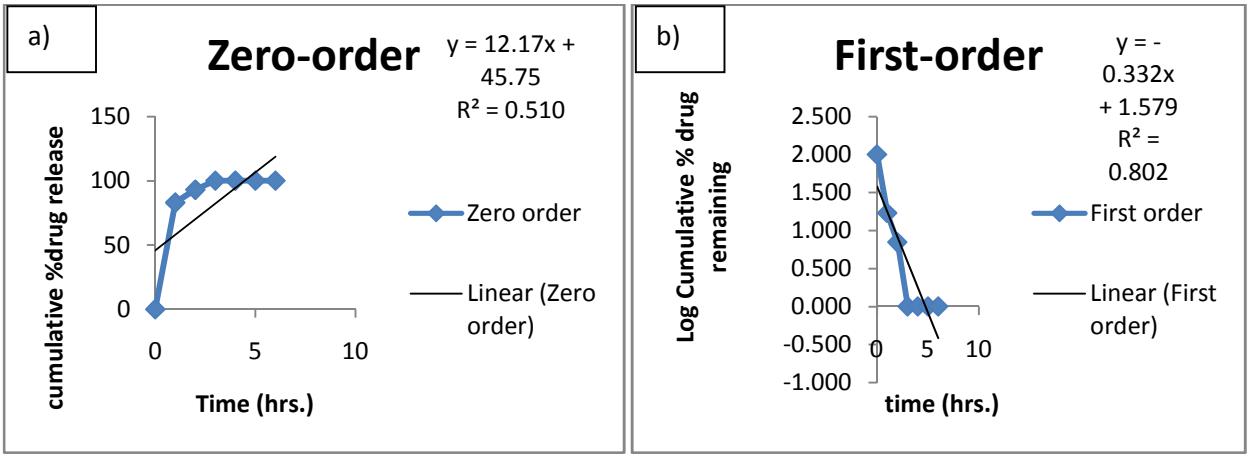

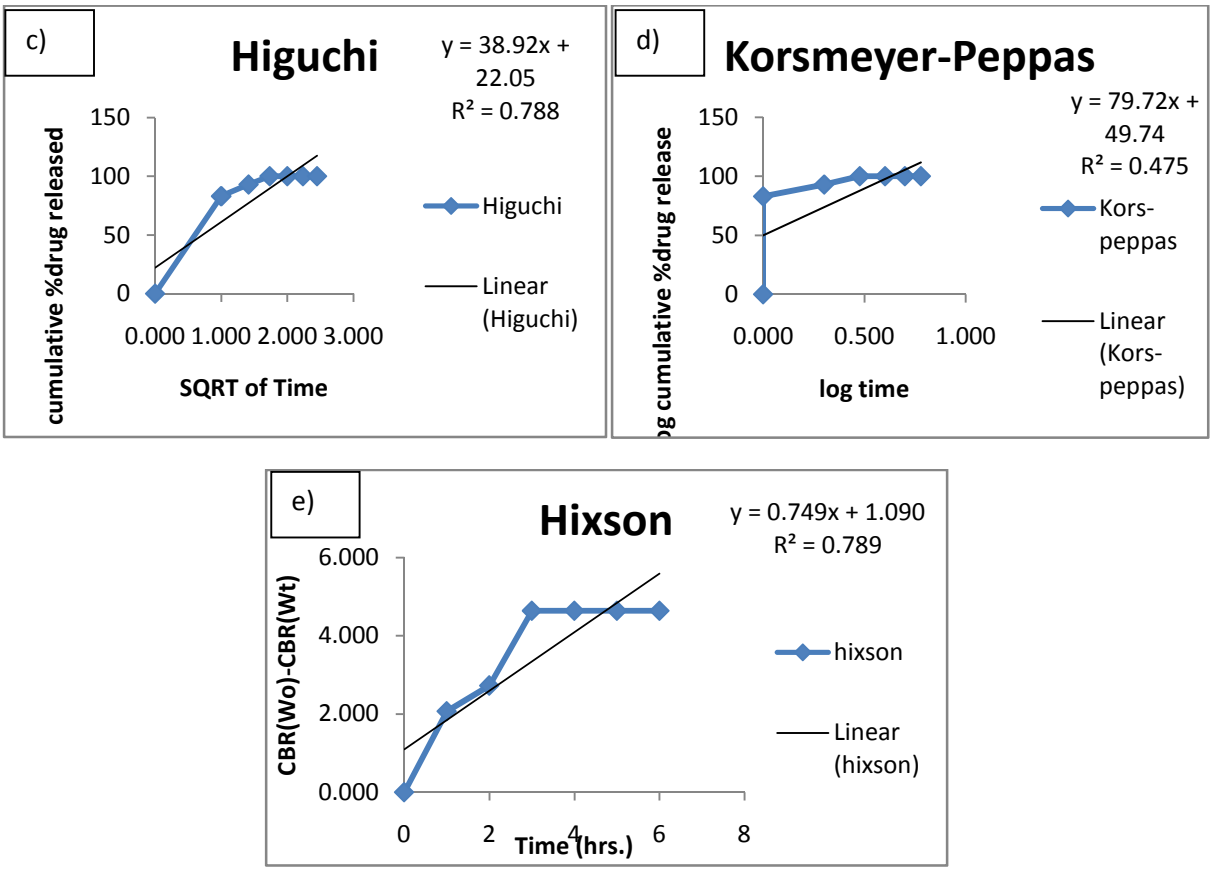

Figure.53: a) Zero-order, b) First-order, c) Higuchi, d) Korsmeyer-Peppas & e) Hixson-Crowell Model for free Ketoconazole.

From the kinetic model plots obtained from the cumulative release data of Ketoconazole from chitosan nanoparticles (Fig 52), it was observed that $\mathbf{R^2}$ (coefficient of correlation) value found to be highest for first-order model (Table.17). Ketoconazole release from chitosan nanoparticles CS1 formulation was only following first-order kinetics. Therefore, it defines that rate of reaction was directly proportional to the concentration of the drug. Other models like Higuchi, Kors-peppas and Hixon used to study the release of water soluble drugs from semi solid matrix, release of drug from swelling as well as non swelling polymeric systems and drug release from systems where there is a change in surface area and diameter of particles respectively (Chime et al., 2013). The values of correlation coefficient of Korsmeyer-Peppas model for the obtained release data was very low (0.705). As mentioned, release exponent of Korsmeyer-Peppas kinetic model describes Ketoconazole release mechanism and depending on its value, release process can be driven by Fickian diffusion (n equal to 0.5), polymeric matrix erosion or the combination of both mechanisms. In Higuchi model, drug releases as a diffusion process based on the Fick's law, square root time dependent and low correlation coefficient value (0.938) described that the drug was not water soluble. In the kinetic modeling of free Ketoconazole release (Fig 53), the highest value of regression coefficient was for first-order model.

4.7.5. Kinetic Models for Ciprofloxacin loaded chitosan nanoparticle formulation (CS1).

Table.19: External Factors Evaluation (EFE) matrix analysis for Ciprofloxacin loaded CS1.

Model Name	Ciprofloxacin loaded CS1		
	R^2	Slope	Intercept
Zero-order model	0.955	14.22	8.271
First-order model	**0.994**	-0.139	2.024
Higuchi model	0.972	36.89	-6.126
Korsmeyer -Peppas model	0.633	1.465	0.847
Hixson-Crowell model	0.993	0.369	0.023

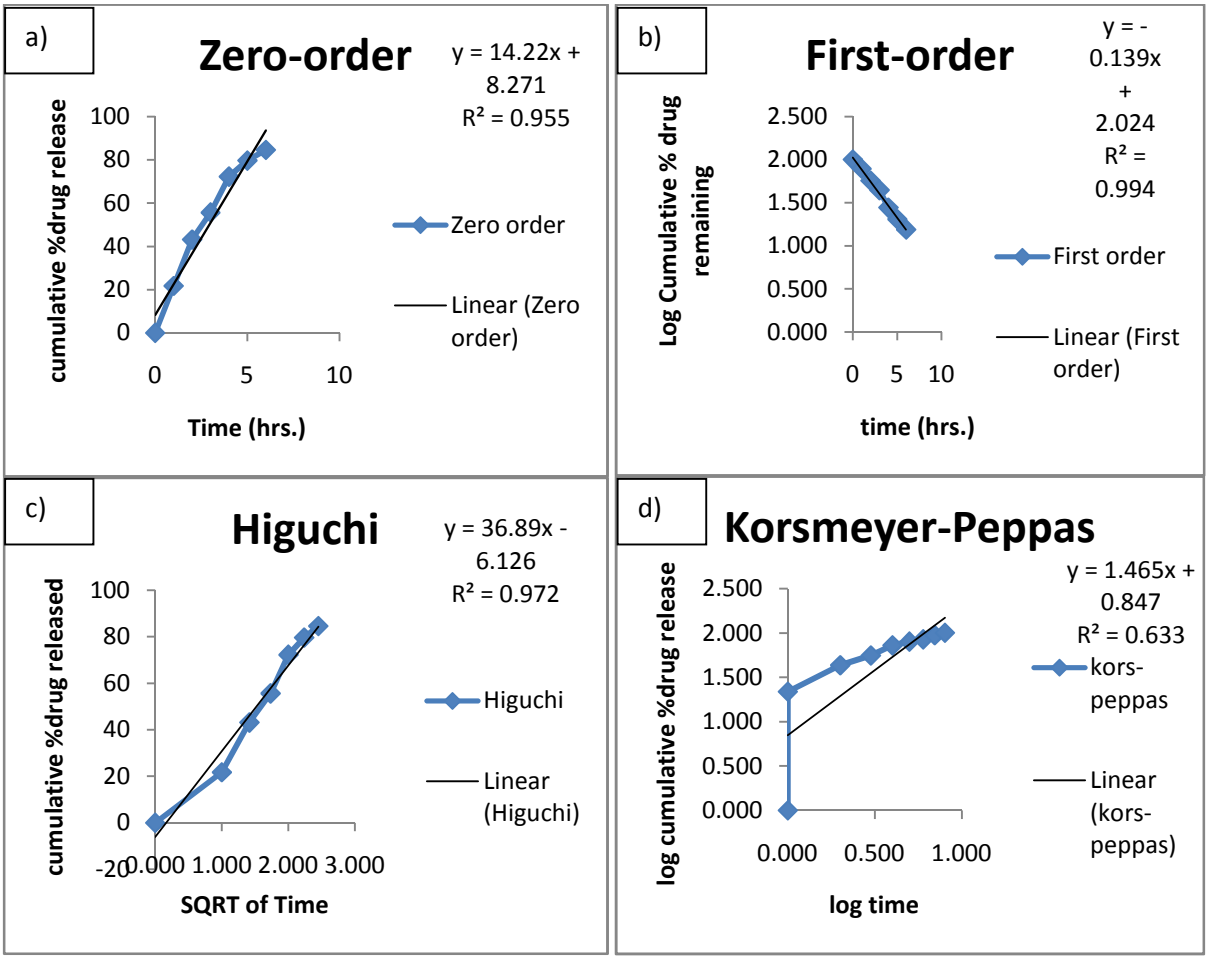

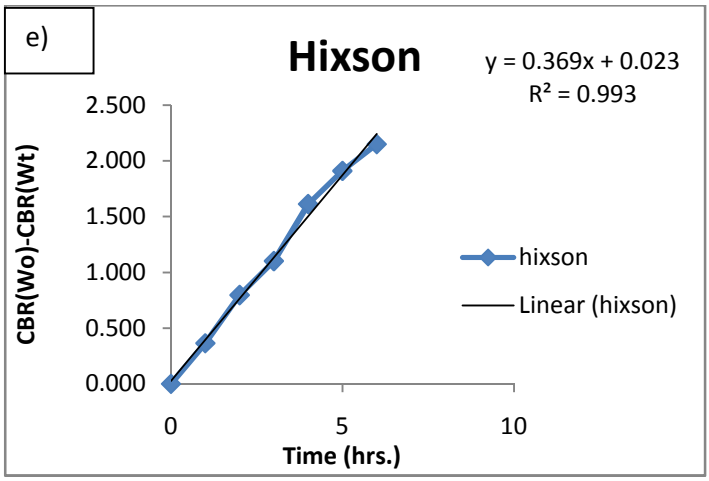

Figure.54: a) Zero-order, b) First-order, c) Higuchi, d) Korsmeyer-Peppas & e) Hixson-Crowell Model for Ciprofloxacin release from Chitosan nanoparticle formulation CS1.

4.7.6. Kinetic Models for Free Ciprofloxacin release.

Table.20: External Factors Evaluation (EFE) matrix analysis for free Ciprofloxacin.

	Free Ciprofloxacin		
Model Name	**R^2**	**Slope**	**Intercept**
Zero-order model	0.615	13.25	39.45
First-order model	**0.903**	-0.36	1.776
Higuchi model	0.868	40.45	16.59
Korsmeyer -Peppas model	0.589	88	43.27
Hixson-Crowell model	0.902	0.803	0.605

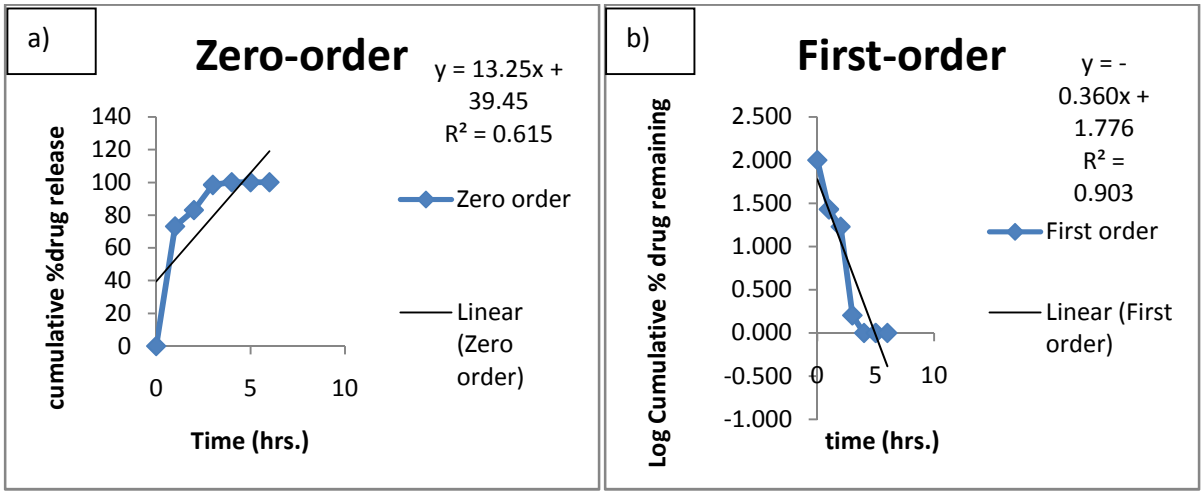

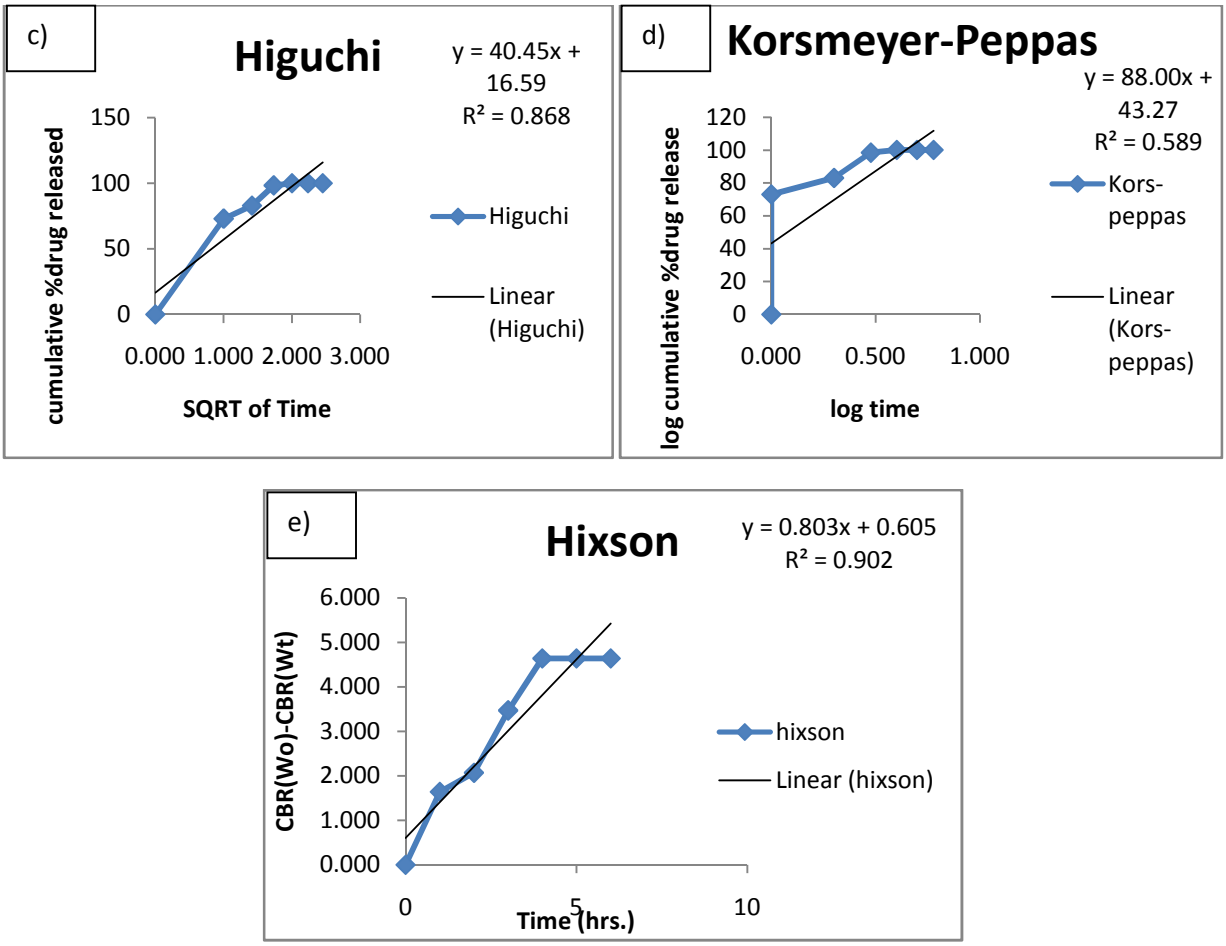

Figure.55: a) Zero-order, b) First-order, c) Higuchi, d) Korsmeyer-Peppas & e) Hixson-Crowell Model for free Ciprofloxacin release.

From the kinetic model plots obtained from the cumulative release data of Ciprofloxacin from chitosan nanoparticles (Fig 54), it was observed that $\mathbf{R^2}$ (coefficient of correlation) value found to be highest for first-order model (Table.19). Ciprofloxacin release from chitosan nanoparticles CS1 formulation was only following first-order kinetics as the regression line or trend line was very close to cumulative drug release profile. Therefore, it defines rate of reaction increases with the increase in drug concentration. First-order kinetics also describes that the release of Ciprofloxacin depends upon its concentration. In the kinetic modeling of free Ciprofloxacin release (Fig 55), it was found that the cumulative release profile of free Ciprofloxacin was not too closer to trend or regression line in any of the model. The highest value of regression coefficient was observed for first-order kinetic model. Other models like Higuchi, Korsmeyer-Peppas and Hixon used to study the release of water soluble drugs from semi solid matrix, release of drug from swelling as well as non swelling polymeric systems and drug release from systems where there is a change in surface area and diameter of particles respectively (Chime et al., 2013).

4.7.7. Kinetic Models for Vancomycin loaded chitosan nanoparticle formulation (CS1).

Table.21: External Factors Evaluation (EFE) matrix analysis for Vancomycin loaded CS1.

Model Name	Vancomycin loaded CS1		
	R^2	Slope	Intercept
Zero-order model	0.958	9.741	8.911
First-order model	**0.985**	-0.075	1.984
Higuchi model	0.973	27.81	-4.061
Korsmeyer -Peppas model	0.691	1.323	0.8
Hixson-Crowell model	0.974	0.226	0.079

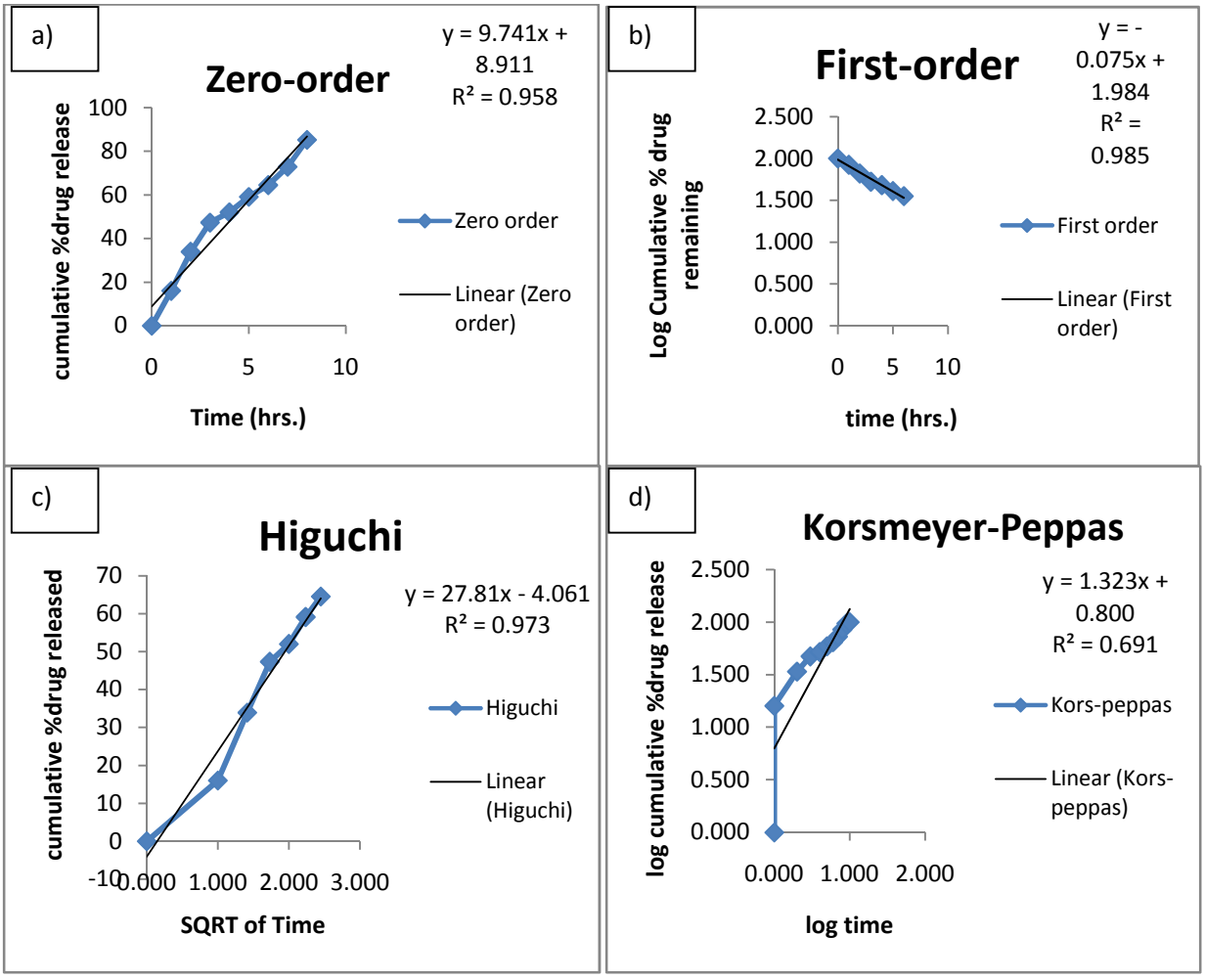

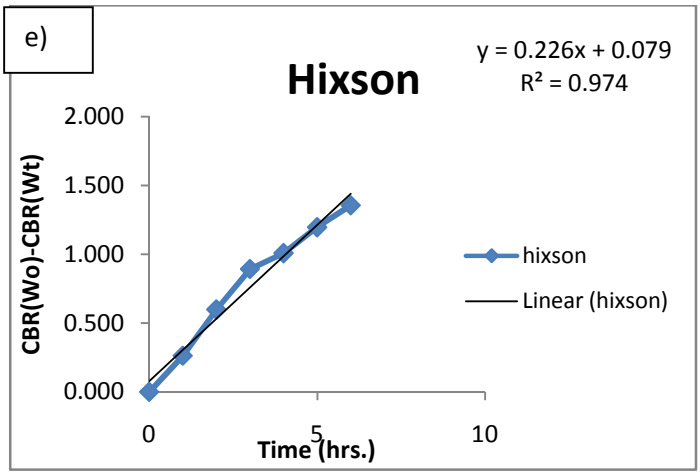

Figure.56: a) Zero-order, b) First-order, c) Higuchi, d) Korsmeyer-Peppas & e) Hixson-Crowell Model for Vancomycin release from Chitosan nanoparticle formulation CS1.

4.7.8. Kinetic Models for free Vancomycin release.

Table.22: External Factors Evaluation (EFE) matrix analysis for free Vancomycin.

	Free Vancomycin		
Model Name	**R^2**	**Slope**	**Intercept**
Zero-order model	0.556	12.63	43.01
First-order model	**0.883**	-0.346	1.661
Higuchi model	0.825	39.54	19.72
Korsmeyer -Peppas model	0.523	83.12	46.98
Hixson-Crowell model	0.882	0.775	0.796

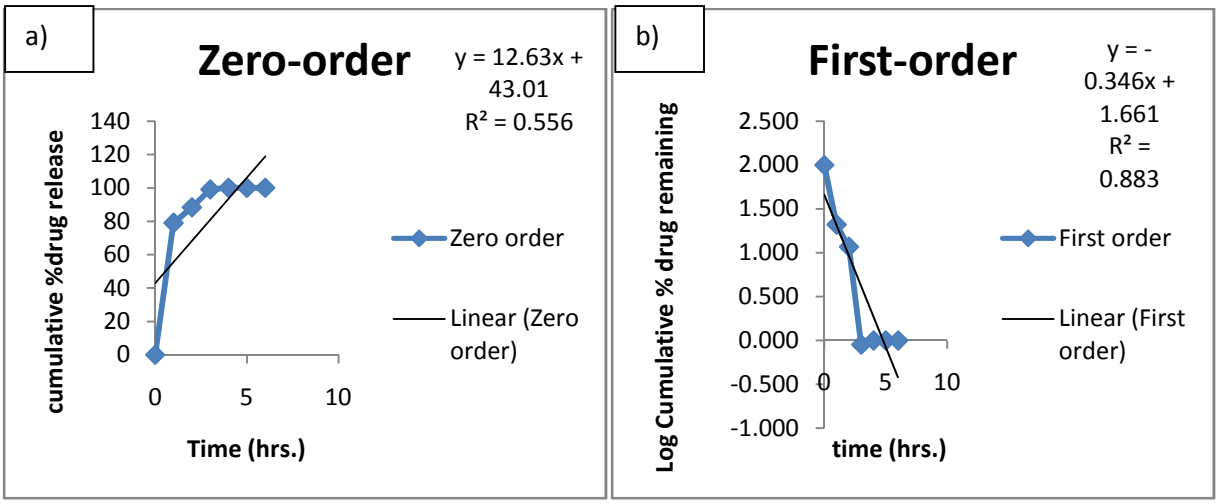

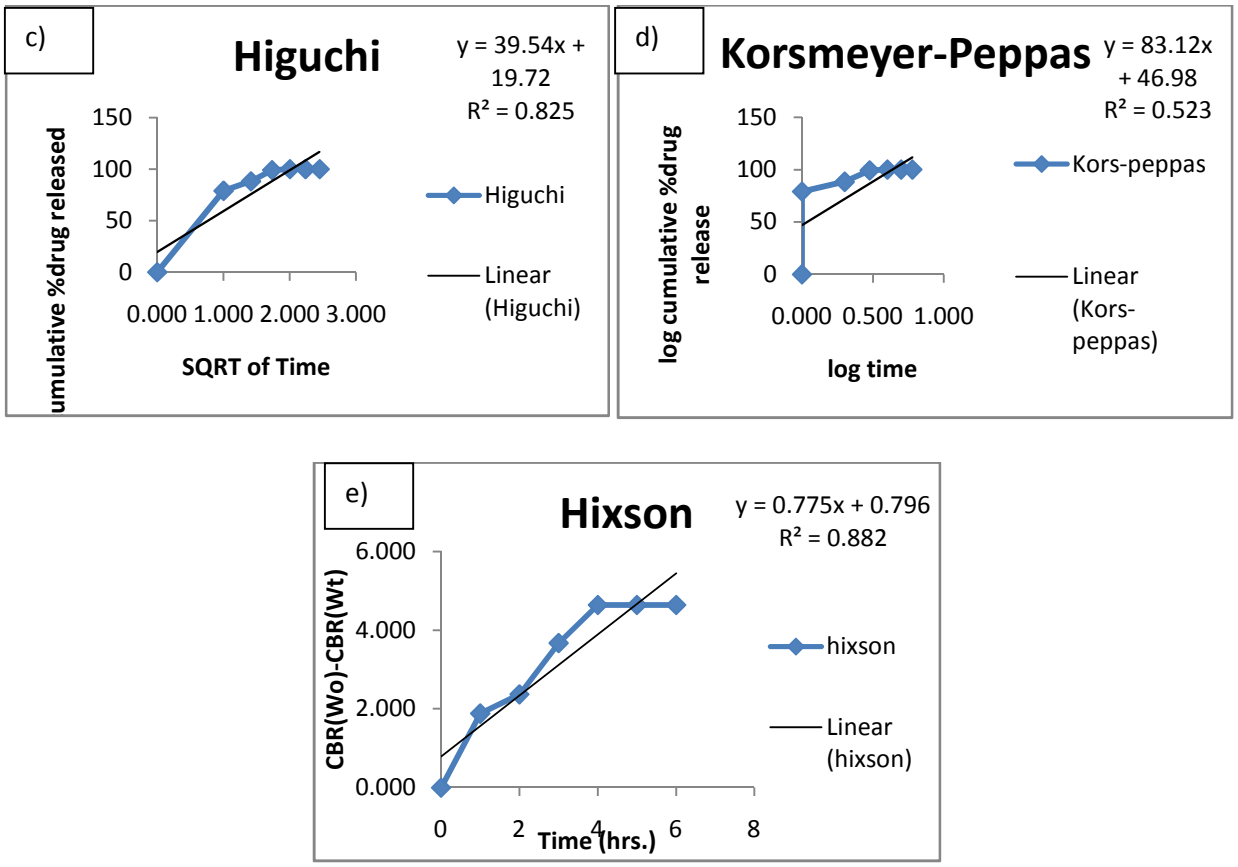

Figure.57: a) Zero-order, b) First-order, c) Higuchi, d) Korsmeyer-Peppas & e) Hixson-Crowell Model for free Vancomycin release.

The kinetic model plots obtained from the cumulative release data of Vancomycin from chitosan nanoparticles (Fig 56), it was observed that $\mathbf{R^2}$ (coefficient of correlation) value found to be highest for first-order model (Table.21). Vancomycin release from chitosan nanoparticles CS1 formulation was best fitted with first-order kinetics. Hixon model used to study the drug release from systems where there is a change in surface area and diameter of particles (Chime et al., 2013). Correlation coefficient value in Hixon model of Vancomycin formulation was low (0.974) as compared to First-order kinetic model; therefore there was no change in surface area or particle's diameter. The values of correlation coefficient of Korsmeyer-Peppas model for the obtained release data was very low (0.691). As mentioned, release exponent of Korsmeyer-Peppas kinetic model describes Vancomycin release mechanism and depending on its value, release process can be driven by Fickian diffusion (n equal to 0.5), polymeric matrix erosion or the combination of both mechanisms. In Higuchi model, drug releases as a diffusion process based on the Fick's law, square root time dependent and low correlation coefficient value (0.973) described that the drug was not water soluble. In the kinetic modeling of free Vancomycin release (Fig 57), the highest value of regression coefficient was for first-order model (Hadžiabdić et al., 2014).

4.7.9. Kinetic Models for Chloramphenicol loaded chitosan nanoparticle formulation (CS1).

Table.23: External Factors Evaluation (EFE) matrix analysis for Chloramphenicol loaded CS1.

Model Name	Chloramphenicol loaded CS1		
	R^2	Slope	Intercept
Zero-order model	0.989	11.16	5.293
First-order model	**0.987**	-0.092	2.02
Higuchi model	0.944	29.91	-6.957
Korsmeyer -Peppas model	0.702	1.345	0.794
Hixson-Crowell model	0.986	0.268	-0.019

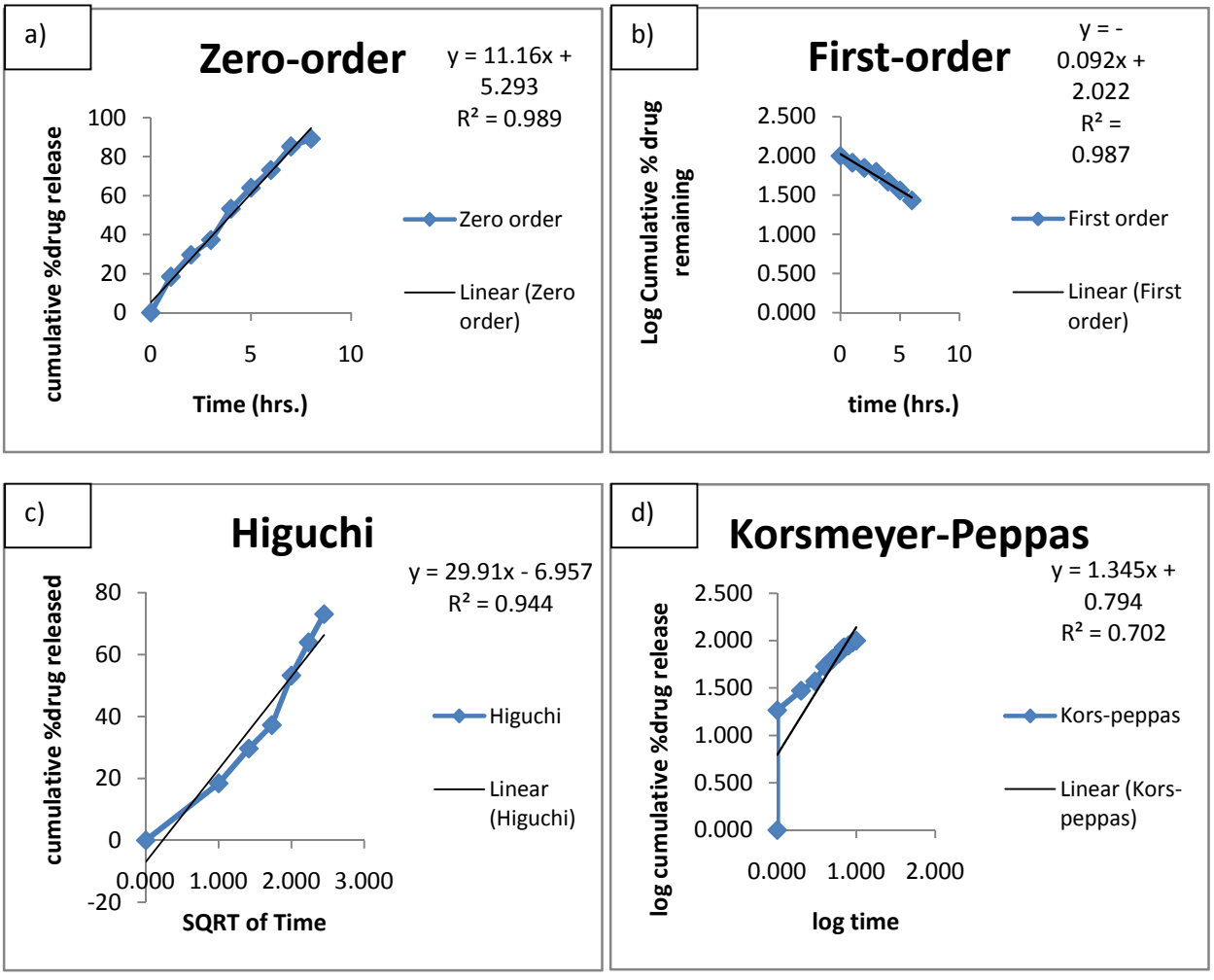

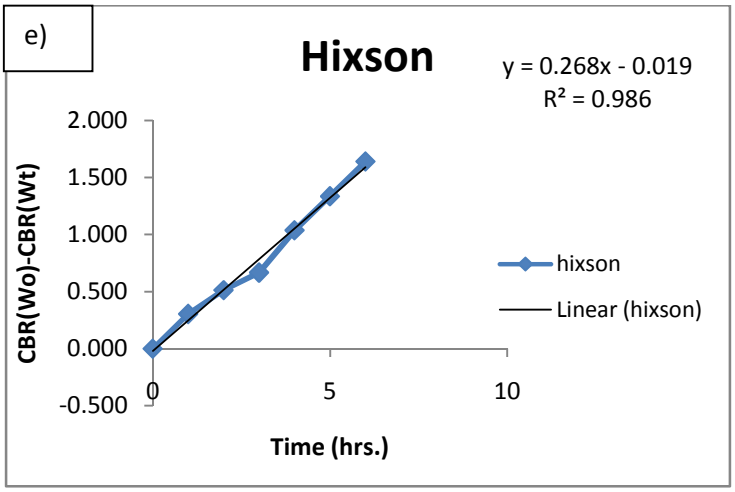

Figure.58: a) Zero-order, b) First-order, c) Higuchi, d) Korsmeyer-Peppas & e) Hixson-Crowell Model for Chloramphenicol release from CS1.

4.7.10. Kinetic Models for Free Chloramphenicol release.

Table.24: External Factors Evaluation (EFE) matrix analysis for free Chloramphenicol.

	Free Chloramphenicol		
Model Name	**R^2**	**Slope**	**Intercept**
Zero-order model	0.597	12.96	40.53
First-order model	**0.912**	-0.355	18.08
Higuchi model	0.854	39.83	17.78
Korsmeyer -Peppas model	0.355	0.987	1.210
Hixson-Crowell model	0.906	0.792	0.601

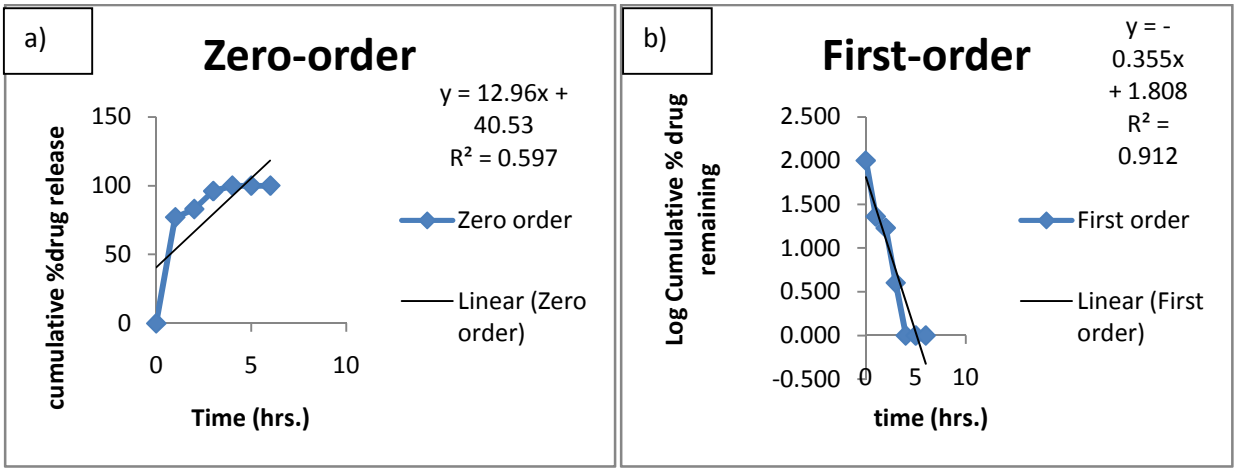

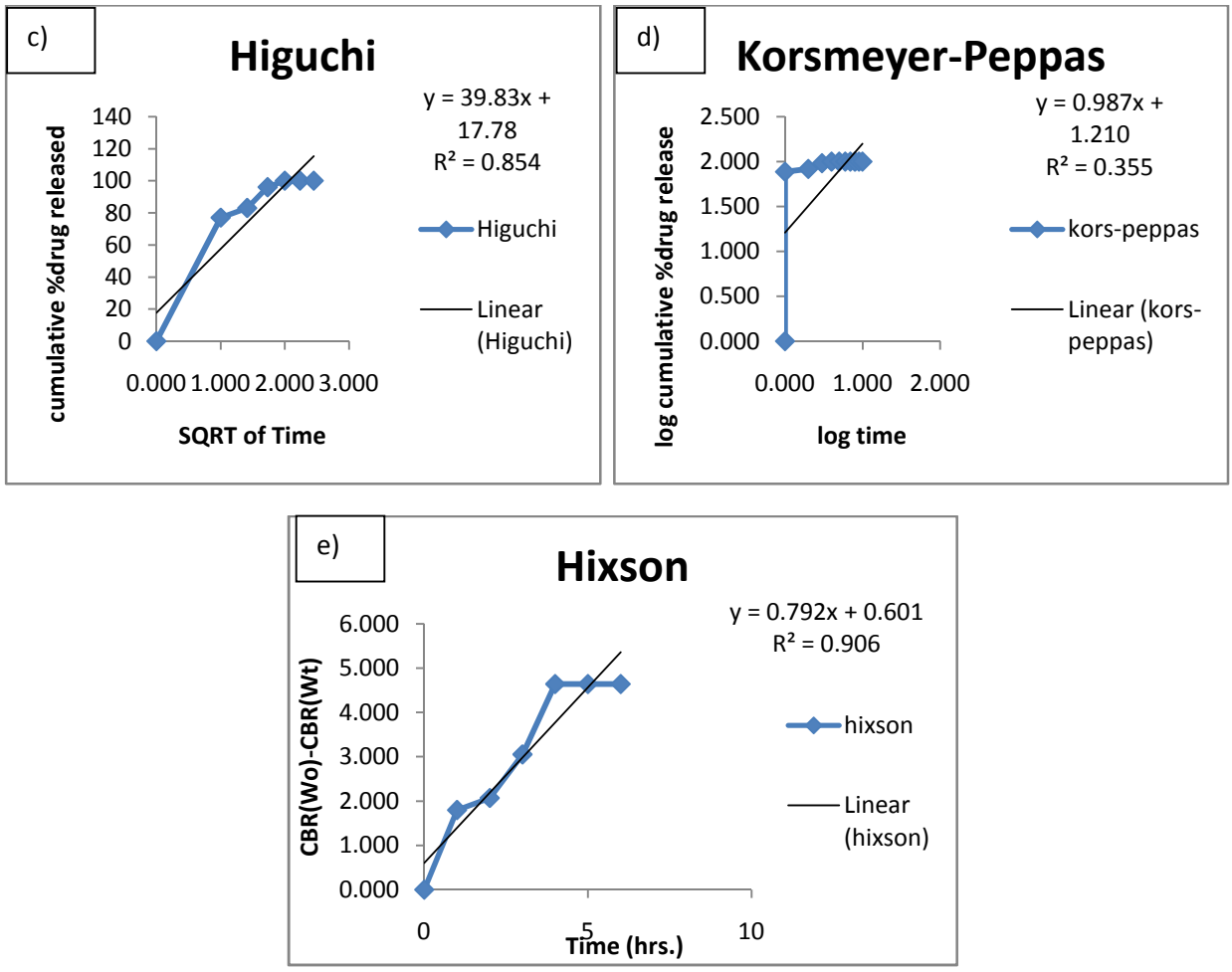

Figure.59: a) Zero-order, b) First-order, c) Higuchi, d) Korsmeyer-Peppas & e) Hixson-Crowell Model for free Chloramphenicol release.

From the kinetic model plots obtained from the cumulative release data of Chloramphenicol from chitosan nanoparticles CS1 formulation (Fig 58), it was observed that $\mathbf{R^2}$ (coefficient of correlation) value found to be highest for first-order model (Table.23). Chloramphenicol release from chitosan nanoparticles CS1 formulation was only following or best fitted to first-order kinetics as the regression line or trend line was very close to the line of cumulative drug release profile. Therefore, it defines rate of reaction increase with the increase in drug concentration. Zero-order kinetics of drug release also describes that the release of Chloramphenicol from chitosan nanoparticle was independent of its concentration of the dissolved substance or drug Chloramphenicol itself. Other models like Higuchi, Korsmeyer-Peppas and Hixon used to study the release of water soluble drugs from semi solid matrix, release of drug from swelling as well as non swelling polymeric systems and drug release from systems where there is a change in surface area and diameter of particles respectively (Chime et al., 2013).

The Hixson-Crowell cube root law describes the release from system where there is a change in surface area and diameter of the particles or tablets. An alteration in the surface area and diameter of the matrix system as well as in the diffusion path length from the matrix drug load occurs during the dissolution process. In Chloramphenicol loaded chitosan nanoparticle formulation CS1 the value of correlation coefficient for Hixon model was low (0.986), therefore it can be assumed that Chloramphenicol was not releasing through dissolution process from chitosan matrix. Release exponent of Korsmeyer-Peppas kinetic model describes Chloramphenicol release mechanism and depending on its value, release process can be driven by Fickian diffusion (n equal to 0.5), polymeric matrix erosion or the combination of both mechanisms. Chloramphenicol chitosan formulation was not following Korsmeyer-Peppas model (0.702) therefore release mechanism occurred by combination of both processes as described. In Higuchi model, drug releases as a diffusion process based on the Fick's law, square root time dependent but low correlation coefficient value (0.973) described that the Chloramphenicol was not water soluble (Hadžiabdić et al.,2014).

In the kinetic modeling of free Chloramphenicol release (Fig 59), it was found that the cumulative release profile of free Chloramphenicol was not too close to trend or regression line in any of the model. The highest value of regression coefficient was obtained for the first-order model. Therefore it could be said that the free Chloramphenicol release kinetics best fitted to the First-order kinetics that means release of the drug was not time dependent.